An Integrated Direct-to-Biology Platform for the Nanoscale Synthesis and Biological Evaluation of PROTACs

Rebecca Stevens[†,‡,#], Enrique Bendito-Moll[†,‡,#], David J. Battersby[†], Afjal H. Miah[†], Natalie Wellaway[†], Robert P. Law[†], Peter Stacey[†], Diana Klimaszewska[†], Justyna M. Macina[†], Glenn A. Burley[‡], John D. Harling[†,*]

[†]Medicinal Chemistry, GSK Medicines Research Centre, Gunnels Wood Road, Stevenage, Hertfordshire, SG1 2NY, United Kingdom

[‡]Department of Pure and Applied Chemistry, University of Strathclyde, 295 Cathedral Street, Glasgow, G1 1XL, United Kingdom

ABSTRACT: Proteolysis targeting chimeras (PROTACs) are heterobifunctional molecules that co-opt the cell's natural proteasomal degradation mechanisms to selectively tag and degrade undesired proteins. However, a challenge associated with PROTACs is the difficult optimisation required to identify new degraders, thus the development of high-throughput platforms for their synthesis and biological evaluation is required. In this study, we establish an ultra high-throughput experimentation (ultraHTE) platform for PROTAC synthesis, followed by direct addition of the crude reaction mixtures to cellular degradation assays without any purification. This 'Direct-to-Biology' (D2B) approach was validated, then exemplified in a medicinal chemistry campaign to identify novel BRD4 PROTACs from a BRD4-binding scaffold previously unexplored for targeted protein degradation. Using the D2B platform, the synthesis of over 600 PROTACs was carried out in a 1536-well plate and subsequent biological evaluation of these candidates was performed by a single scientist in less than one month, to identify a set of picomolar BRD4 degraders. Due to its ability to hugely accelerate the optimisation of new degraders, we anticipate our platform to transform the synthesis and testing of PROTACs.

INTRODUCTION

Proteolysis Targeting Chimeras (PROTACs) are a rapidly evolving modality, currently sparking great excitement within the pharmaceutical industry. Since the first report of a PROTAC in 2001[1] to the present, 18 of these potential drugs are already in clinical evaluation[2] for a range of different indications.[3, 4]

PROTACs are made up of two distinct small-molecule binders, an E3 ubiquitin ligase ligand and protein-of-interest (POI) ligand, connected *via* a linker. By forming a ternary complex between the PROTAC, E3 ligase and POI, these proteins are brought into close proximity to each other, resulting in ubiquitination of the POI. This tags the POI for targeted protein degradation by the proteasome.

One key advantage of PROTACs is the opportunity to target traditionally 'undruggable' targets *via* an event-based mechanism of action (MoA) that co-opts the cell's own protein degradation machinery to degrade a specific POI.[5] This event-based MoA additionally benefits from sub-stoichiometric quantities of drug being sufficient to degrade the target protein,[6] as well as a disconnect between POI binder affinity and degradation extent due to the potential for ternary complex cooperativity, with examples of low-affinity ligands being incorporated into potent degraders.[7]

However, the significantly larger and more complex structures of PROTACs, with Beyond Rule of 5 (bRo5) physicochemical properties,[8] leads to challenges in compound synthesis and purification. Additionally, slight changes to the structure can have a large impact on biological activity or physicochemical properties.[9, 10] Despite initial efforts being made towards the

rational design of new PROTACs,[11, 12] an empirical approach is needed to identify hit and lead compounds.

As such, new methods to accelerate the rate of PROTAC synthesis and optimisation are required.[13] Herein, we report a high-throughput chemistry platform for PROTAC synthesis and biological testing of crude compounds, completely eliminating the need for any purification – a method termed 'Direct-to-Biology' (D2B).[14] This approach removes a key bottleneck in the optimisation process, delivering cellular degradation data in very short turnaround times. Ultimately, optimal use of the platform allows us to interrogate a wide section of chemical space for a given protein-of-interest in a single experiment.

In 2015, Merck published an ultrahigh-throughput experimentation (ultraHTE) approach,[15] where a plate-based synthetic platform and associated biochemical ASMS assays were integrated to accelerate the drug discovery process of kinase inhibitors. Inspired by this work, we sought to achieve the same throughput but extending biological evaluation to cell-based assays in the context of targeted protein degradation. Janssen recently reported a platform to accelerate PROTAC synthesis with multistep amide coupling chemistry, only purified using cartridges, and highlighted how this could be used to assess crucial structure-activity relationships (SAR) in the PROTAC space.[16] Whilst this approach is indeed much faster than iterative synthesis, purification was still required using this approach. Tang and co-workers have taken crude PROTAC-containing reaction mixtures from acylhydrazone or phthalimidine formations into cell-based evaluation.[17, 18] However, this chemistry is limited to reactions with no additional

reagents and water as the sole by-product, to form PROTACs with non-desirable physicochemical properties that require further optimisation and resynthesis of analogues with different linking functionalities. As such, we propose an integrated approach which directly links PROTAC synthesis with biological evaluation, using crude reaction mixtures for the facile SAR profiling of PROTAC candidates in a streamlined fashion (Figure 1).
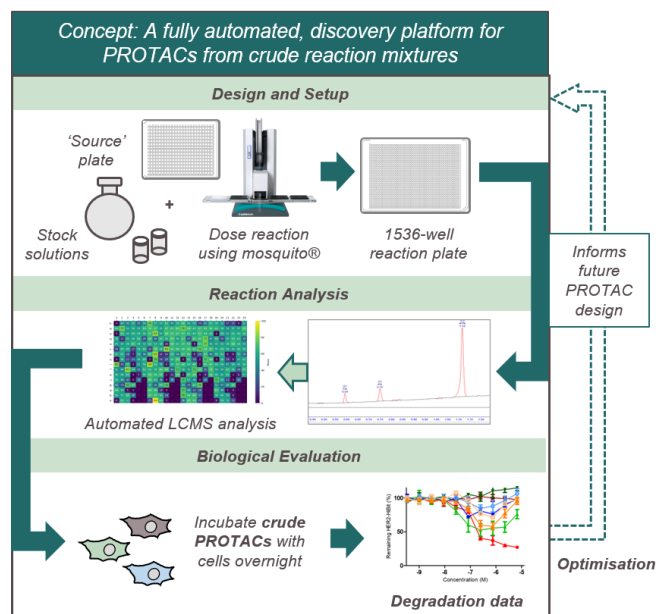
Figure 1: D2B platform developed for PROTAC synthesis and direct biological assay to deliver cellular degradation data for large libraries of compounds within two weeks of preparing the starting material stock solutions. Stock solutions are dosed onto a 384-well plate then a mosquito® liquid handling robot doses out the 1536-well reaction plate; an aliquot is taken for LCMS and results are analysed by PyParse[19, 20]; successful reactions are taken to cellular assay without further purification; compounds of interest are resynthesised for further profiling and SAR informs the next iteration of compound design.

Proof of concept and platform validation
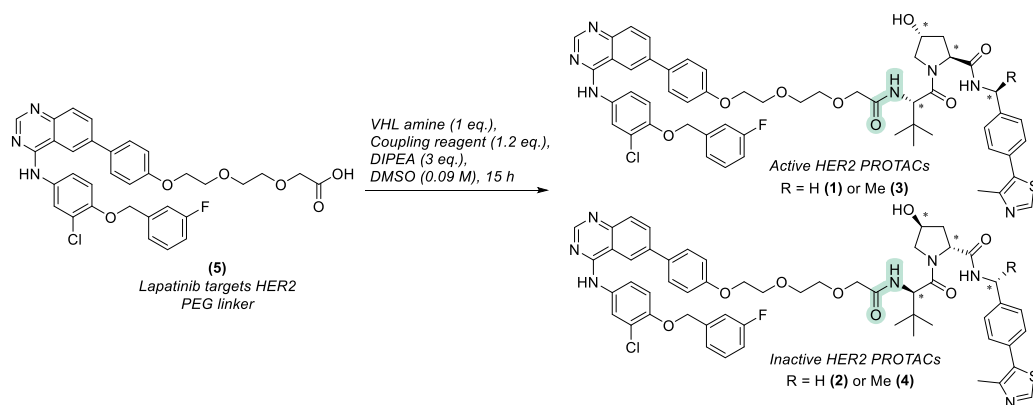
The primary goal in the development of the PROTAC D2B workflow was to incorporate automation at each step of the process. With the mosquito® liquid handling robot, we were able to select 1536-well plates for chemistry as microfluidic mixing eliminated the need to stir or shake the plate.[15] Furthermore, miniaturisation to 5 µL reaction mixtures and only 150 nmol of material would allow for the most efficient use of advanced chemical intermediates, and safer handling.[21, 22]

For initial proof of concept work, a previous PROTAC design was used to benchmark the platform. This was a lapatinib-based HER2 targeting PROTAC **1** and its inactive enantiomer **2** reported by Crews *et al.*[23] (Figure 2). An additional pair of PROTACs **3** and **4** where R = Me were added as controls, for additional validation and potential improvements in potency.[24]
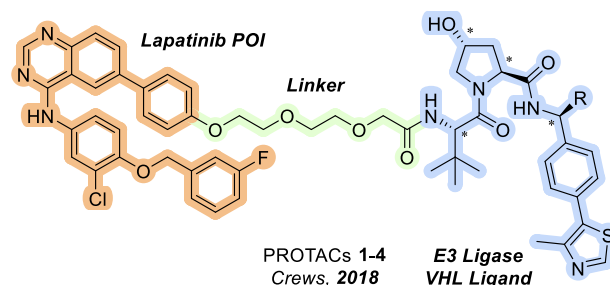
Figure 2. Lapatinib-based HER2-targeting PROTAC reported by Crews et al[23]; compound chosen as a model system for development of new amide coupling conditions for PROTAC D2B synthesis. R = H or methyl; reversal of VHL E3 ligase stereocentres (marked as *) provides inactive control compounds.

The linkage chemistry we chose to investigate for the preparation of PROTACs in a plate format was an amide coupling. For biological assessment, a HiBiT assay was selected to quantify protein degradation.[25] This can be performed in 384-well plate format,[26] and could be further integrated with the 1536-well plate chemistry workflow. A Cell-Titer-Glo (CTG) assay was used to assess cell viability; this was required to ensure that reagents involved in the reactions performed were not generating false positives due to cytotoxicity.

Synthesis of the HER2-VHL PROTACs was utilised for the chemistry optimisation work, with reaction between the HER2-PEG acid **5** and a VHL amine (Scheme 1).

Scheme 1: Optimisation of the nanoscale amide coupling reaction

HER2 acid **5** was reacted with 4 VHL amines where R = H/Me with both active (as drawn) and inactive (stereocentres * reversed) enantiomers of the VHL ligand to give 4 HER2-targeting PROTACs **1**, **2**, **3** and **4**.

2

First, seven common amide coupling reagents were evaluated (EDC, DIC, HATU, TSTU, TCFH, PDCP and COMU) on PROTACs **1-4**. High conversion to PROTAC was observed by LCMS with HATU and EDC (Table S1). When these reaction mixtures were assessed in the HER2 HiBiT assay, both HATU and EDC conditions gave a similar degradation profile to the control **1** (Figure 3a). However, HATU showed a dose-dependent decrease in the cell viability (Figure 3b). As this could lead to misleading results in the degradation assay and give false positives, HATU was avoided and instead EDC was selected due to its high conversion to PROTAC by LCMS and absence of cytotoxicity by CTG when the PROTAC reaction mixtures were tested. During the optimisation phase of PROTAC synthesis, it was noticed that DIPEA was not miscible with DMSO in 5 µL reaction mixtures. Exchanging the base from DIPEA to NMM resulted in homogenous reaction mixtures, and NMM showed no cytotoxicity by CTG assay (Figure S2).

A) HER2-HiBiT degradation assay (n=3)

1 - purified
3 - purified
1 - D2B with EDC
3 - D2B with EDC
1 - D2B with HATU
3 - D2B with HATU

B) CTG assay (n=3)

1
1 - D2B with EDC
3 - D2B with EDC
EDC - no PROTAC
1 - D2B with HATU
3 - D2B with HATU
HATU - no PROTAC
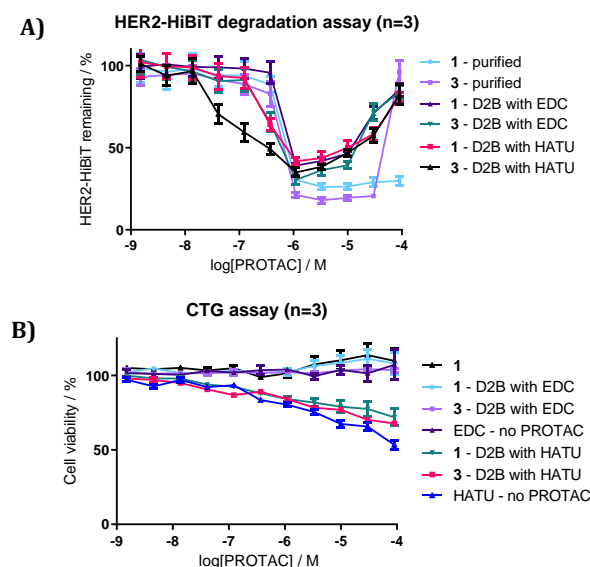
Figure 3. Optimal exemplar reactions from the amide coupling reagent screen to prepare PROTACs **1** and **3** were assessed in the HiBiT and CTG assays; purified PROTACs and individual coupling reagents were added as controls; error bars indicate standard error over 3 technical replicates.

When using these conditions with EDC, formation of a suspected *N*-acylurea by-product was observed (Scheme S1), so to minimise this formation a range of additives were investigated to minimise this competing pathway (Table S2).[27] HOAt, HOBt, NHS and OxymaPure were screened in the CTG assay, and whilst the benzotriazole reagents reduced cell viability, NHS and OxymaPure resulted in no cytotoxicity. OxymaPure was highly effective at increasing conversion so final conditions were chosen using EDC as the coupling reagent, NMM as the base and OxymaPure as the additive to reduce side-product formation.

The selected conditions were then assessed with a range of relevant amines to investigate the robustness of the chemistry. High conversion (80-100%) to the desired PROTAC product was observed with primary, secondary, hindered and non-hindered amines (Figure S1). The only challenging group found in assessing the scope was an aniline with an amide group in the meta position, where only partial (30%) conversion was observed, but *para*-chloroaniline was well tolerated with 90% conversion to the desired product.

Once the chemistry conditions were in hand, a library of HER2 degrading PROTACs was designed using a 29 member library of E3 ligase-linker amines with HER2-targeting acids **5** and **6**, including the positive and negative controls reported by Crews *et al.* (Scheme 2). An aliquot of each reaction mixture was analysed by LCMS (Table S3) and reactions that showed full consumption of the limiting reagent were deemed to have sufficient PROTAC purity to progress to the degradation assay.

Scheme 2. Library synthesis of HER2-targeting PROTACs using optimised D2B conditions
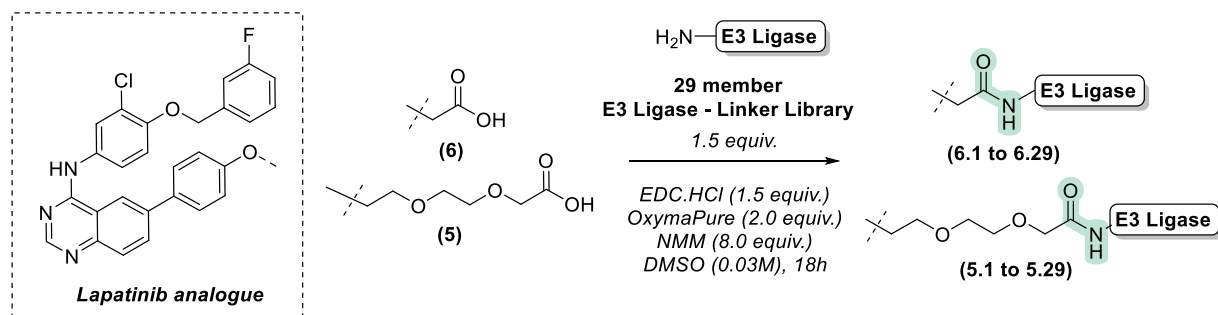
Optimisation of the amide coupling resulted in a final set of conditions, which were applied to acids **5** and **6** to generate a library of 58 lapatinib-based HER2 PROTACs.

The control PROTACs gave the expected degradation profiles and the *in situ* synthesised controls showed similar degradation and cytotoxicity profiles to the isolated samples (Figure 4a and c). A more pronounced hook effect was observed with the D2B positive control than the purified sample, which may be rationalised by the presence of excess binder competing with the PROTAC at higher concentrations.

From the library, several novel HER2 PROTAC hits were identified: **5.2**, **5.7**, **6.2** and **6.7** (Figure 4b). Two of these were resynthesised (**6.2** and **6.7**) and mechanistic experiments were carried to confirm targeted degradation (Figure 4d-g).

A proteasome-impaired degradation assay was run with the addition of epoxomicin to prove that an active proteasome is required to observe degradation upon addition of PROTAC. Reduction in HER2-HiBiT protein levels was not observed in the cells that had been treated with epoxomicin (Figure 4d-e). Next, competition experiments were conducted with addition of excess E3 ligase ligand; the addition of excess VHL binder prevented HER2-HiBiT degradation in a dose-dependent manner, indicating that binding to VHL is essential for the PROTACs to induce degradation of the POI (Figure 4f-g).
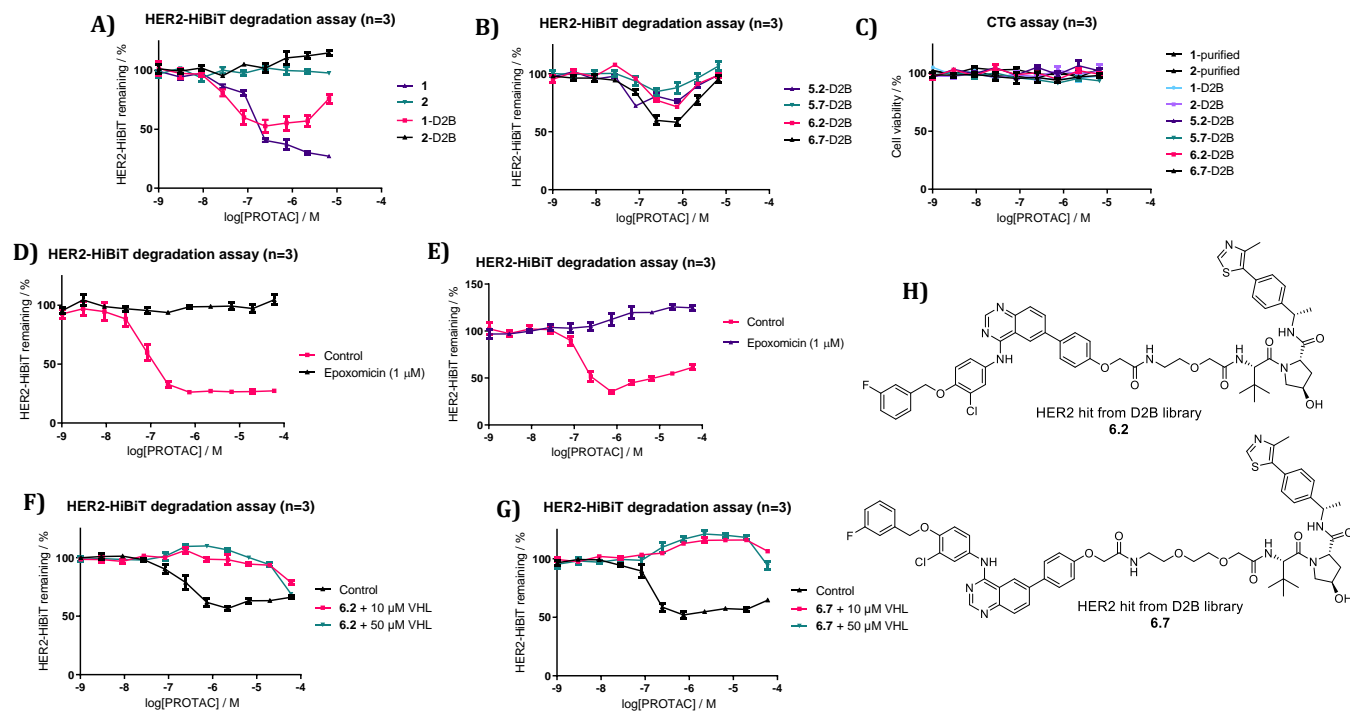
Figure 4: a) Isolated and D2B samples for the previously reported PROTACs **1** and **2** showed comparable degradation profiles; b) 4 novel HER2 PROTAC hits were identified from the library; c) None of the samples tested compromised cell viability in the CTG assay; d) to e) Degradation of HER2-HiBiT does not occur in the presence of **6.2** (d) or **6.7** (e) in combination with proteasome inhibitor epoxomicin, giving evidence that degradation is proteasome-mediated; f) to g) competition experiments with PROTAC **6.2** (f) and **6.7** (g) with increasing concentrations of VHL ligand show that degradation requires binding to VHL; h) chemical structures of novel hits **6.2** and **6.7**; error bars indicate standard error over 3 technical replicates.

In summary, we established a nanoscale plate-based coupling and biological evaluation platform for PROTAC profiling. Furthermore, novel HER2 PROTAC hits were identified and validated, indicating that the platform could robustly identify new hits. The next goal was to apply this to a novel POI binder to perform a medicinal chemistry campaign using the D2B approach.

Application of the platform to BRD4

Next, we aimed to apply the platform in the identification of novel BRD4 PROTACs. Whilst compounds based on BRD4 binder JQ1 are potent degraders,[5] the JQ1 binder is highly lipophilic (ChromlogD$_{7.4}$ = 7.3). We hypothesised that starting from I-BET469 **7**, a BRD4 BD1-selective binder developed in our laboratories with improved physicochemical properties (ChromlogD$_{7.4}$ = 2.6),[28] would result in BRD4 PROTACs that have more desirable physicochemical properties. Furthermore, this compound had not been used in a PROTAC previously.

X-ray crystallography of I-BET469 **7** was used to identify two solvent exposed regions, establishing potential exit vector sites from the benzimidazole-based BRD4 binder (Figure 5). Furthermore, the morpholine ring projects through the ZA channel and its terminal oxygen does not make any interactions with BRD4, thus it was hypothesised that it could be replaced without losing potency. The branched dimethoxypropane makes simultaneous contacts with the ZA loop and WPF shelf, but as this is a solvent exposed region and alternative substituents were also tolerated at this vector, we decided that these were good starting points for introduction of a PROTAC linker. Utilising these two exit vectors, three carboxylic acid intermediates **8 – 10** were synthesised, from which a library of 186 BRD4-targeting PROTACs (62 per vector) were made and tested *via* D2B amide coupling chemistry.

PROTACs with the morpholine exit vector and the presence of the piperidine ring (i.e., vector 1a) gave a much higher hit rate than other vectors and were more potent degraders than PROTACs based on the other two scaffolds. The morpholine exit vector without the piperidine ring gave a lower hit rate, but many potent compounds were still identified. Vector 2 only gave a small number of degrader hits and many compounds tested were inactive, indicating that this exit vector does not tolerate as many groups as vector 1, and thus is not as suitable for PROTAC linkers. This highlights the ability of D2B to take a previously unexplored POI binder and scope out multiple exit vectors simultaneously to identify the most promising for further optimisation.
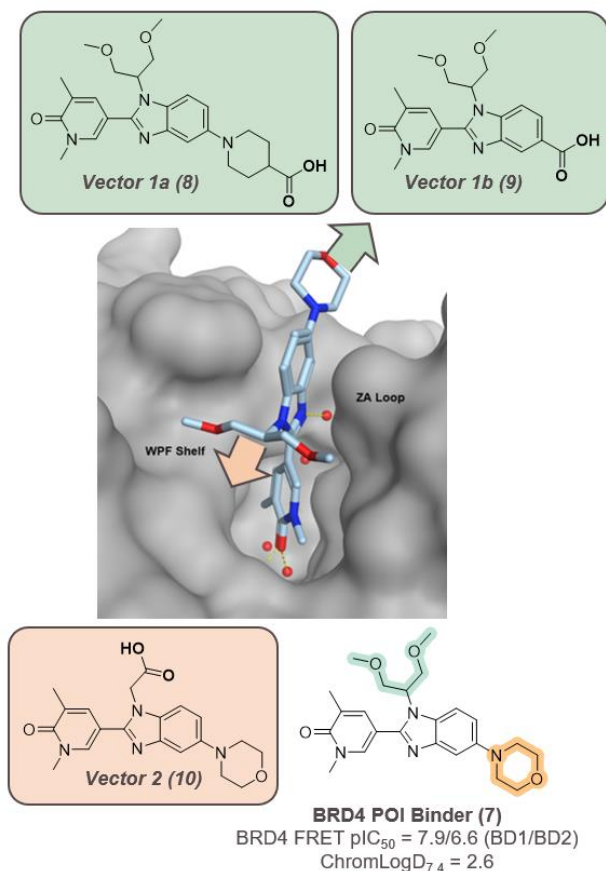
Figure 5: X-ray crystallography of BRD4 POI Binder **7** identified two solvent exposed regions, from which three structural analogues with PROTAC exit vectors were designed and synthesised; PDB 6TPZ.

Some of the most potent compounds did show a decreased cell viability of 20-30%, but the degradation observed in the HiBiT assay was significantly larger and thus the activity could be attributed to the PROTAC degradation capacity, as opposed to being cell viability related (Figure 7b). It was hypothesised that this drop in cell viability with only the most active PROTACs was in fact caused by the total loss of BRD4 protein at higher concentrations of PROTAC.

As with the HER2 proof of concept work, 18 hits were resynthesised and purified. All showed excellent correlation with the D2B data (Figure 6). This array demonstrated the platform's utility to rapidly assess the suitability of a novel binder as a PROTAC warhead, as the synthesis of this D2B library was carried out by one scientist within 72 hours and required less than 10 mg of starting material.
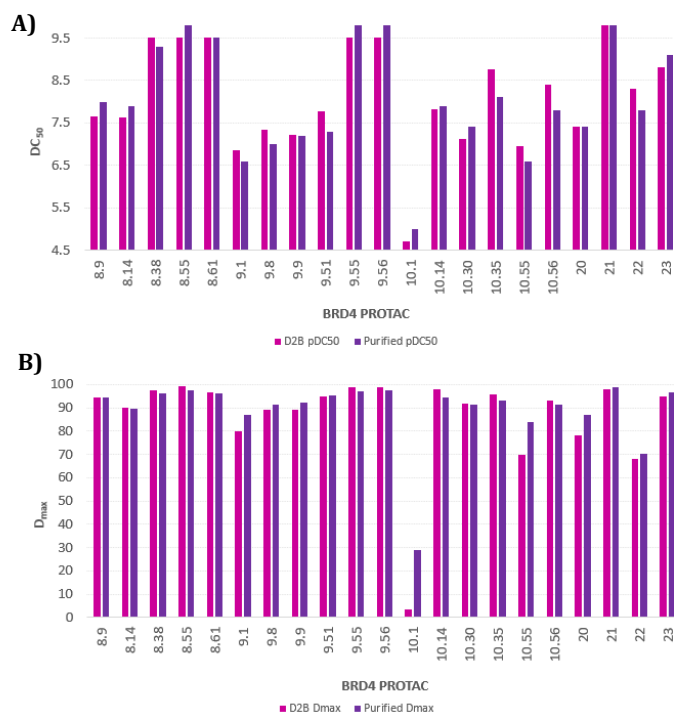
Figure 6. 18 BRD4 PROTACs were resynthesised and degradation data for the purified compounds showed excellent correlation with D2B data. Mean of technical duplicates for the D_{max} and absolute pDC_{50} are used; compounds with $pDC_{50} > 9.7$ or < 4.7 are given this numerical value for the purposes of comparison.

Mechanistic investigations were carried out with vector 2 hit **10.30** (see SI for results with **8.36** and **9.46**) to confirm a proteasome-mediated response was observed from the BRD4 PROTACs. Repeating the epoxomicin experiment gave consistent results to HER2 experiments, indicating that the BRD4-HiBiT degradation is proteasome-mediated (Figure 7). Addition of excess E3 ligase binder (lenalidomide in this example) reduced degradation of the POI in a dose-dependent manner, although to a smaller extent than in the HER2 example. This was likely due to the PROTAC's high potency; the target is degraded even when just a small fraction of the molecules bind to BRD4. This data, combined with the HER2 competition experiments, indicates that a small excess of E3 ligase binder from incomplete reaction conversion does not prevent the identification of new hits by D2B, although for some targets the degradation observed may be less than that of the purified sample if substantial quantities of E3 ligase binder are present.

5

A) BRD4-HiBiT degradation assay (n=3)

- Control
- **10.30** + 1 µM Lenalidomide
- **10.30** + 10 µM Lenalidomide

x-axis: log[PROTAC] / M
y-axis: BRD4-HiBiT remaining / %

B) BRD4-HiBiT degradation and CTG assay (n=3)

- CTG – Control
- Degradation – Control
- CTG – Epoxomicin
- Degradation – Epoxomicin

x-axis: log[PROTAC] / M
y-axis: BRD4-HiBiT remaining / %; cell viability
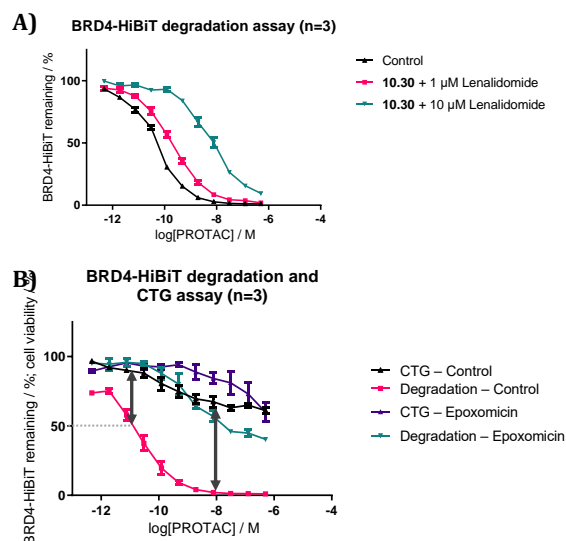
Figure 7. Mechanistic experiments with PROTAC **10.30;** a) competition with increasing concentrations of lenalidomide; b) addition of proteasome inhibitor epoxomicin; error bars indicate standard error over 3 technical replicates.

Once the ideal exit vector and some basic SAR was gained from these experiments, a much larger D2B experiment was designed. Starting from the bromobenzimidazole intermediate **11** a small library of short linkers were installed at the exit vector from the bromobenzimidazole core *via* late-stage $C(sp^2)$-$C(sp^3)$ cross-coupling chemistry to give **12.1**-**12.8** (Scheme 3). It was envisioned that this linkage would not only provide a more rigid compound and favour formation of a productive ternary complex, but also eliminate a metabolic hotspot at the POI-linker connection.[29] The small library of BRD4-linker intermediates were rapidly purified by mass-directed auto purification (MDAP), then subjected to deprotection conditions to give **13.1**-**13.8**, at which stage they were ready for D2B.

Scheme 3: Synthesis of over 600 PROTACs in one D2B experiment
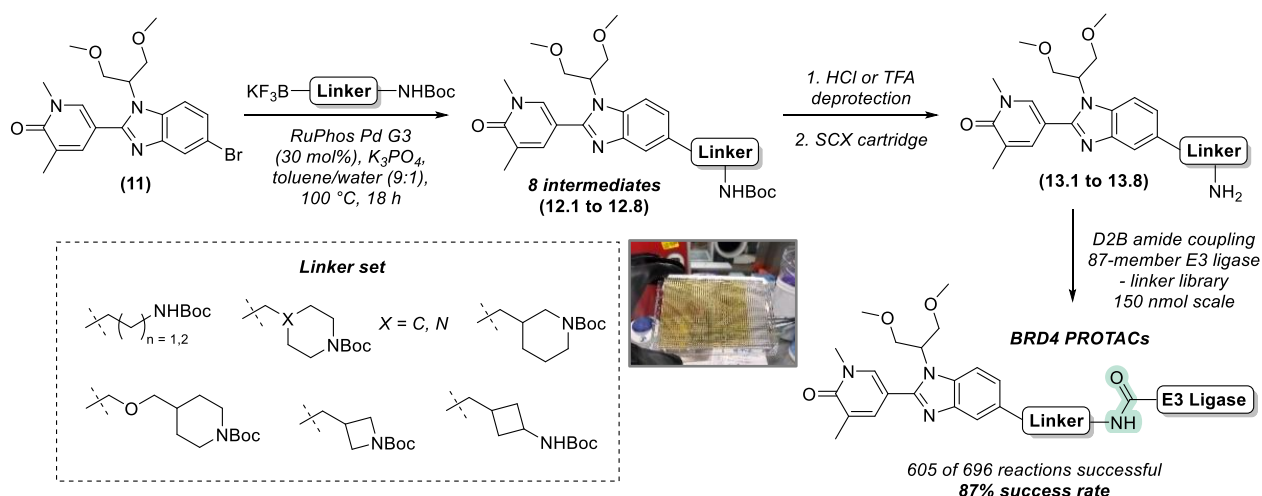
Synthetic route to 605 novel BRD4 PROTACs, with a chemistry success rate of 87% in the D2B reaction; array synthesis was employed to synthesise the required intermediates for generation of a diverse library.

The D2B amide coupling chemistry between the POI amines and E3 ligase-linker acid library gave an excellent success rate of 87%, providing a library of over 600 compounds. At this point, the development of PyParse at GSK allowed for automated LCMS analysis.[19, 20] Within minutes of inputting the raw LCMS file and a list of PROTACs, purities for the full library were automatically generated and the successful reaction mixtures could be diluted for biological assay. As with the HER2 library, reaction mixtures with full consumption of the limiting reagent (in this case the POI-targeting amine) were progressed into the assay. The additional automation in the LCMS analysis step saved an estimated 6 hours of chemist's time in what would otherwise be a manual assessment of nearly 700 reaction mixtures.

The compounds were tested by HiBiT, and a selection assessed by CTG. Most of the compounds tested were highly potent, with many pico- to nanomolar BRD4 degraders observed. Several PROTACs with picomolar activity were identified, but as seen in the initial scoping of SAR, these highly potent compounds did give a drop in cell viability at the highest concentration, indicating that if all HiBiT-BRD4 protein is removed from these cells, the cell viability is affected. However, these highly potent compounds ($pDC_{50} > 10.77$) degraded to the top limit of the concentration range in the assay, and are amongst the most potent BRD4 degraders reported in the literature.[30, 31]

Some broad trends were identified within the library; PROTACs with cereblon and VHL-mediated degradation were observed to be active, but initial analysis of SAR showed that cereblon PROTACs were typically more potent than VHL. An optimal linker length of 12-15 atoms was observed, with particularly long or short linkers generally having a lower pDC_{50}, although exceptions to this were seen. Both flexible linkers e.g., with PEG or carbon chains, and semi-constrained e.g. with saturated heterocycles or aromatic groups, were tolerated. Given the size of the library, further analysis using computational methods will aid in the selection of top compounds to profile further. Compound resynthesis and investigation of drug-like

6

properties is under investigation and will be the subject of a future publication.
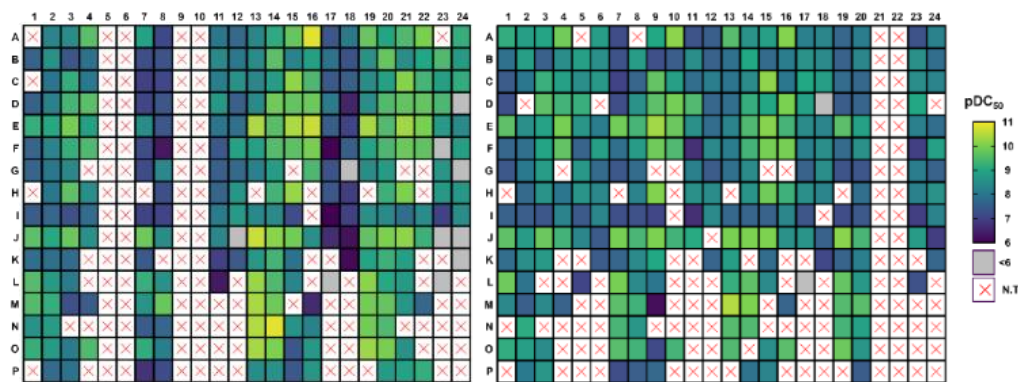
Figure 8: Platemap of compounds; heatmap coloured by pDC_{50} of tested compounds; assay pDC_{50} range was 6 to 10.77; N.T. represents compounds that were not tested in the HiBiT assay; platemap layout corresponds to LCMS conversion in Figure S3.

This experiment demonstrated the ability to explore a wide array of chemical space in a single data-rich experiment, which can inform future PROTAC design. Less than 0.1 mg was required for each PROTAC to be synthesised, meaning that for D2B with an 87 member E3 ligase-linker acid library, only 10 mg of each intermediate was required. This highlights the value of directly testing nanoscale reactions in the assay, as compound throughput has been increased approximately 100-fold. Furthermore, the full library including high-throughput array to generate the starting materials, D2B synthesis and compound assay was carried out by a single chemist in a combined time of under a month. Compared to bespoke synthesis, this timeline is hugely accelerated - synthesis of over 600 similar PROTACs through singleton synthesis and small arrays could easily take a year or more with a multitude of chemists.

Conclusion

In summary, the D2B platform offers the opportunity to overcome the challenges in PROTAC optimisation and obtain large amounts of data for a medicinal chemistry campaign in just a few experiments. The huge resource savings of this approach can be integrated with computational chemistry to further streamline PROTAC designs, ranging from new POI/E3 ligase binders through to linkerology-based approaches. Ultimately, the development of a bespoke PROTAC-specific platform of automated and integrated workflows has accelerated and increased the throughput of PROTAC screening.

Further work is currently ongoing to profile top hits from the BRD4 libraries and to expand the repertoire of D2B transformations for PROTAC synthesis. We anticipate these to be the topics of future disclosures.

EXPERIMENTAL SECTION

General Information

Solvents and reagents were purchased from commercial suppliers and used as received. If not commercially available, compounds were prepared according to the literature unless stated otherwise. Reactions were carried out under nitrogen and stirred using a magnetic stirrer hotplate unless stated otherwise. Reactions using the glovebox were carried out in an MBraun MB-200B glovebox with an inert N_2 atmosphere. Automated column chromatography was performed using a Teledyne ISCO CombiFlash® Rf with premade RediSep® silica cartridges.

Materials, Reagents and Analytical

NMR spectra were recorded at ambient temperature using standard pulse methods on a Bruker AV-400 instrument at 400 MHz, a Bruker AV4 at 700 MHz or a Bruker AVIIIHD at 600 MHz. Chemical shifts (δ) are reported in parts per million (ppm). Peak assignments were chosen based on chemical shifts, integrations, and coupling constants, considering 2D analyses where necessary, or the following solvent peaks: CDCl$_3$ (^{1}H = 7.27 ppm), DMSO-d_6 (^{1}H = 2.50 ppm), CD$_3$OD (^{1}H = 4.87 and 3.31 ppm) or DMF-d_7 (^{1}H = 8.03, 2.92 and 2.75 ppm). Coupling constants are quoted to the nearest 0.1 Hz and multiplicities are given by the following abbreviations and combinations thereof: s (singlet), d (doublet), t (triplet), q (quartet), quin (quintet), sxt (sextet), m (multiplet), br. (broad). The purity of all biologically tested compounds was ≥95% as determined by LCMS UV traces except for **8.55** (93% purity), **9.51** (92% purity), **9.55** (94% purity), **10.14** (92% purity), **10.35** (88% purity), **10.55** (81% purity), **10.56** (87% purity) but these were deemed sufficient for comparison with the crude D2B samples. LCMS analysis was carried out on a Waters Acquity UPLC instrument equipped with a BEH column (50 mm x 2.2 mm, 1.7 μm packing diameter) and Waters micromass ZQ MS using alternate-scan positive and negative electrospray. Analytes were detected as a summed UV wavelength of 210 – 350 nm. Two liquid phase methods were used:

Formic – 40 °C, 1 mL/min flow rate. Gradient elution with the mobile phases as (A) water containing 0.1% (v/v) formic acid and (B) acetonitrile containing 0.1% formic acid. Gradient conditions were initially 1% B, increasing linearly to 97% B over 1.5 min, remaining at 97% for 0.1 min then increasing to 100% B over 0.1 min.

High pH – 40 °C, 1 mL/min flow rate. Gradient elution with the mobile phases as (A) 10 Mm aqueous ammonium bicarbonate solution, adjusted to pH 10 with 0.88 M aqueous ammonia and (B) acetonitrile. Gradient conditions were initially 1% B, increasing linearly to 97% B over 1.5 min, remaining at 97% B for 0.4 min then increasing to 100% B over 0.1 min.

MDAP purification was performed on a Waters FractionLynx system comprising of a Waters 600 pump with extended pump heads, Waters 2700 autosampler, Waters 996 diode array and Gilson 202 fraction collector. HPLC separation was conducted

7

on a Xselect CSH C18 column (150 mm x 30 mm internal diameter, 5 μm packing diameter) at ambient temperature, eluting with ammonium bicarbonate or formic acid aqueous solutions with acetonitrile using an appropriate elution gradient determined by LCMS analysis. Mass spectra were recorded on a Waters ZQ mass spectrometer using alternate-scan positive and negative electrospray ionisation with a 150-1000 amu scan range, 0.5 s scan time with an 0.2 s inter-scan delay.

Biology Protocols

HiBiT and CellTitre-Glo® assays

Degradation of proteins of interest (POIs) in cells treated with PROTACs was quantified using the Nano-Glo® HiBiT Lytic Detection System (Promega) in 384 well assay plate format. Clonal cell lines were first established in which the gene was modified using CRISPR/Cas9 editing, so the encoded protein included a HiBiT peptide tag. The HiBiT BRD4 cell line was HEK with N-terminal tag and the HER2 HiBIT cells were HeLa with C-terminal tag. 10 mM DMSO stock solutions of PROTACs were prepared and diluted across an 11 concentration, 3 fold increment range. Typically 25 nL or 50 nL was dispensed into a white opaque bottomed 384 well assay plate using an acoustic ECHO dispenser (Labcyte). For assay, cells were detached from culture flasks using TrypLE Express enzyme and centrifuged at 400g for 5 min. The cell pellet was resuspended in assay medium (FluoroBrite™ DMEM supplemented with 10% heat inactivated FBS, GlutaMAX™ , penicillin 50U/mL and streptomycin 50ug/mL). Alternatively cryopreserved assay ready aliquots of cells were used which were prepared in advance and stored at -150 °C in 90% FBS/10% DMSO. 25 μL of cell suspension containing 10,000 cells was dispensed into each well of the assay plate, which was then incubated for 18 h at 37 °C /5% CO_2. Control wells were included, with assay medium without cells being the no POI remaining 100% effect control and cells treated with DMSO vehicle only, the 0% effect control. 25 μL of Nano-Glo® HiBiT lysis buffer supplemented with LgBiT protein and Nano-Glo® substrate was added to each well and the plate shaken at 500 rpm for 10 min at room temperature. Luminescence intensity was measured using a PHERAstar microplate reader (BMG Labtech) and the % POI remaining in each well calculated by normalizing the raw luminescence value to the above control wells. Parameters corresponding to the potency and efficacy estimates of the PROTACs were obtained from these values using software (IDBS ActivityBase and GraphPad Prism). Two versions of the DC_{50}, called relative DC_{50} and absolute DC_{50} were typically generated corresponding to the inflection point of a fitted 4-parameter sigmoidal response curve and the interpolated concentration of PROTAC corresponding to 50% of the protein degraded, respectively. The D_{max} parameter was the maximum experimentally observed degradation. Proteasome block was achieved by pre-treating cells with 1uM epoxomicin for 1 hour before assays. E3 ligase ligand competition was done by including Lenalidomide **S6** or VHL binder **S8** in the assay at the stated concentration. All cell culture items and the assay plates were from Thermofisher.

The effects of PROTACs on cell viability were estimated by measuring cellular ATP levels using the CellTiter-Glo® Luminescent Cell Viability Assay (Promega). ATP assays were typically conducted with HiBiT assays on a separate assay plate on the same day, following the same general procedure detailed above.

Chemistry

Optimisation of Reaction Conditions

Stock solutions of reagents were prepared in DMSO and manually plated onto a 384-well source plate. The desired volumes of each reagent were then transferred from the source plate into either 384- or 1536-well plates using the Mosquito Liquid Handler, sealed, and left to stand. An aliquot of each reaction mixture was transferred to a 384-well plate, quenched with a solution of internal standard with acetic acid and acetonitrile, then analysed by LCMS. A 3-fold incremental 11-point dilution series was prepared and the daughter plates were run in the HiBiT and CTG assays.

An example of the reaction mixtures prepared during the chemistry optimisation is detailed in Table 1.

Table 1. Example D2B optimisation experiment

Reagent	Eq.	Stock solution	
		Concentration (M)	Volume dispensed (μL)
NHS ester	1.2	0.028	10.7
VHL binder	1	0.023	10.8
DIPEA	4	0.387	2.6
HATU	1.2	0.237	1.3
Sufficient DMSO was added to bring the total volume to 25 μL			

Direct-to-Biology Standard Protocol

Direct-to-Biology reaction mixtures are dispensed into 1536-well microtitre plates using a mosquito® Liquid Handler in the glovebox under inert N_2 atmosphere. Reactions are carried out in 5 μL DMSO at a concentration of 30 mM and are left overnight in a sealed plate without stirring or agitation.

After 18 to 24 h, an aliquot of 0.5 μL of reaction mixture is taken and diluted with 39.5 μL of acetic acid in acetonitrile for LCMS analysis on 2 min Formic method. PROTAC purity is determined by % area in the LCMS UV trace thus is not the same as conversion or product concentration. PyParse is used to automate the analysis process, with the raw data file input and spreadsheet of LCMS purity output.

Compounds are diluted with DMSO and dispensed into columns 1 and 13 of a 384-well assay plate, then a 3-fold incremental 11-point dilution series of each reaction mixture is prepared. Compounds are then tested in the relevant biological assay as crude reaction mixtures. A series of compounds from each D2B experiment are resynthesised with purification and full characterisation to validate biological assay results.

The following reagents are used for the amide coupling transformation: 0.15 μmol of amine made up to 1.5 μL with DMSO per well (0.1 M, 1 eq.), 0.15 μmol of acid made up to 1.5 μL with DMSO per well (0.1 M, 1 eq.), 0.225 μmol of EDC.HCl made up to 1.28 μL with DMSO per well (0.176 M, 1.5 eq.), 0.3 μmol of OxymaPure made up to 0.589 μL with DMSO per well (0.509 M, 2 eq.), 131 nL neat NMM per well (8 eq./1.2 μmol).

Synthesis of intermediates

2-(4-(4-((3-Chloro-4-((3-fluorobenzyl)oxy)phenyl)amino)quinazolin-6-yl)phenoxy)acetic acid (6)

A suspension of *N*-(3-chloro-4-((3-fluorobenzyl)oxy)phenyl)-6-iodoquinazolin-4-amine (850 mg, 1.34 mmol) in a mixture of 1,2-dimethoxyethane (7.7 mL) and ethanol (5.8 mL) was

evacuated under vacuum and purged with nitrogen (x3). Then, a 2 M aqueous solution of sodium carbonate (6.7 mL, 13.45 mmol) was added and the reaction mixture was purged with nitrogen (x3). T*ert*-butyl 2-(4-(4,4,5,5-tetramethyl-1,3,2-dioxaborolan-2-yl)phenoxy)acetate (494 mg, 1.479 mmol) and Pd(PPh$_3$)$_4$ (117 mg, 0.101 mmol) were added to the reaction mixture and the resulting suspension was stirred overnight at 80 °C. The reaction mixture was partitioned between ethyl acetate (80 mL) and water (80 mL), the aqueous phase was back extracted with ethyl acetate (80 mL), the organics were combined, washed with brine (80 mL), passed through a hydrophobic frit and concentrated under reduced pressure to afford the crude product (1.20 g). The crude *tert*-butyl 2-(4-(4-((3-chloro-4-((3-fluorobenzyl) oxy)phenyl)amino)quinazolin-6-yl)phenoxy)acetate (1.20 g, 1.54 mmol) was stirred in TFA (8.90 mL, 115 mmol) for 30 minutes at room temperature. The reaction mixture was concentrated under reduced pressure. The crude product was purified by reverse-phase column chromatography (30-85% acetonitrile-H$_2$O + 0.1% formic acid modifier) and the appropriate fractions concentrated and freeze-dried over 72 h to afford the title product (326 mg, 0.560 mmol, 36% yield over two steps) as a yellow solid. LCMS (Formic): R$_t$ = 0.99 min, [M+H]$^+$ 530.1, 100% purity. ^{1}H NMR: (400 MHz, DMF-d_7) δ ppm 10.03 (s, 1 H), 8.78 (d, J = 1.4 Hz, 1 H), 8.66 (s, 1 H), 8.30 (s, 1 H), 8.25 (d, J = 2.4 Hz, 1 H), 8.22 (dd, J = 8.8, 1.7 Hz, 1 H), 7.88 - 7.95 (m, 2 H), 7.84 (br d, J = 8.5 Hz, 2 H), 7.53 (td, J = 8.0, 5.8 Hz, 1 H), 7.39 - 7.46 (m, 3 H), 7.36 (d, J = 9.0 Hz, 1 H), 7.22 (td, J = 8.3, 2.4 Hz, 1 H), 7.15 (s, 1 H), 5.33 - 5.38 (m, 2 H), 4.85 (s, 2 H).

BRD4 Intermediates

1-(1-(1,3-Dimethoxypropan-2-yl)-2-(1,5-dimethyl-6-oxo-1,6-dihydropyridin-3-yl)-1*H*-benzo[*d*]imidazol-5-yl)piperidine-4-carboxylic acid (8)

Tert-butyl 1-(1-(1,3-dimethoxypropan-2-yl)-2-(1,5-dimethyl-6-oxo-1,6-dihydropyridin-3-yl)-1*H*-benzo[*d*]imidazol-5-yl)piperidine-4-carboxylate (360 mg, 0.686 mmol) was dissolved in TFA (1.5 mL, 19.47 mmol) and stirred at room temperature for 2 h. The solvent was dried under a stream of nitrogen and the crude purified by MDAP (TFA modifier) to afford the title product (360 mg, 0.691 mmol, 100% yield). LCMS (Formic): R$_t$ = 0.53 min, [M+H]$^+$ 469.2, 94% purity. ^{1}H NMR: (400 MHz, DMSO-d_6) δ ppm 8.21 - 8.26 (m, 1 H), 7.99 (d, J = 9.3 Hz, 1 H), 7.68 (dd, J = 2.7, 1.2 Hz, 1 H), 7.34 (m, 2 H), 4.98 (dt, J = 8.8, 4.4 Hz, 1 H), 4.06 (dd, J = 10.5, 9.1 Hz, 2 H), 3.79 (dd, J = 10.8, 4.4 Hz, 2 H), 3.67 - 3.74 (m, 2 H), 3.56 (s, 3 H), 3.19 (s, 6 H), 3.12 (br d, J = 13.2 Hz, 2 H), 2.52 - 2.58 (m, 1 H), 2.11 (s, 3 H), 2.02 (br d, J = 10.8 Hz, 2 H), 1.78 (br d, J = 10.8 Hz, 2 H).

1-(1,3-Dimethoxypropan-2-yl)-2-(1,5-dimethyl-6-oxo-1,6-dihydropyridin-3-yl)-1*H*-benzo[*d*]imidazole-5-carboxylic acid, lithium salt (9)

Methyl 1-(1,3-dimethoxypropan-2-yl)-2-(1,5-dimethyl-6-oxo-1,6-dihydropyridin-3-yl)-1*H*-benzo[*d*]imidazole-5-carboxylate (2.60 g, 6.51 mmol) was stirred in an aqueous solution of lithium hydroxide (65.1 mL, 130 mmol) at 60 °C for 4 h. The reaction mixture was partitioned between mildly acidic water (200 mL, acetic acid, pH 5) and DCM (200 mL). The aqueous phase was washed with DCM (200 mL) six further times, the organics combined and concentrated under reduced pressure to afford the title product (2.08 g, 5.30 mmol, 81% yield) as a white solid. LCMS (Formic): R$_t$ = 0.67 min, [M+H]$^+$ 386.1, 100% purity. ^{1}H NMR: (400 MHz, DMSO-d$_6$) δ ppm 8.19 - 8.23 (m, 1 H), 8.12 (d, J = 1.9 Hz, 1 H), 7.91 - 7.96 (m, 1 H), 7.83 - 7.88 (m,

1 H), 7.66 - 7.72 (m, 1 H), 4.90 (dt, J = 9.0, 4.2 Hz, 1 H), 4.05 (dd, J = 10.2, 8.8 Hz, 2 H), 3.79 (dd, J = 10.5, 4.6 Hz, 2 H), 3.55 (s, 3 H), 3.17 (s, 6 H), 2.10 (s, 3 H).

2-(2-(1,5-Dimethyl-6-oxo-1,6-dihydropyridin-3-yl)-5-morpholino-1*H*-benzo[*d*]imidazol-1-yl)acetic acid (10)

A solution of *tert*-butyl 2-(2-(1,5-dimethyl-6-oxo-1,6-dihydropyridin-3-yl)-5-morpholino-1*H*-benzo[*d*]imidazol-1-yl)acetate (150 mg, 0.342 mmol) in neat TFA (1.00 mL, 13.6 mmol) was stirred at room temperature for 3 h. The reaction mixture concentrated under reduced pressure and purified by MDAP (Formic) to afford the title product (125 mg, 0.327 mmol, 96% yield). LCMS (Formic): R$_t$ = 0.47 min, [M+H]$^+$ 383.2, 100% purity. ^{1}H NMR: (400 MHz, DMSO-d_6) δ ppm 8.21 - 8.25 (m, 1 H), 7.71 (d, J = 9.2 Hz, 1 H), 7.65 (dd, J = 2.4, 1.4 Hz, 1 H), 7.28 (dd, J = 9.2, 2.4 Hz, 1 H), 7.14 (d, J = 1.9 Hz, 1 H), 5.32 (s, 2 H), 3.77 - 3.82 (m, 4 H), 3.55 (s, 3 H), 3.16 - 3.22 (m, 4 H), 2.10 (s, 3 H).

Tert-butyl 1-(1-(1,3-dimethoxypropan-2-yl)-2-(1,5-dimethyl-6-oxo-1,6-dihydropyridin-3-yl)-1*H*-benzo[*d*]imidazol-5-yl)piperidine-4-carboxylate (14)

5-(5-Bromo-1-(1,3-dimethoxypropan-2-yl)-1*H*-benzo[*d*]imidazol-2-yl)-1,3-dimethylpyridin-2(1*H*)-one (390 mg, 0.928 mmol), DavePhos (18.26 mg, 0.046 mmol), tris(dibenzylideneacetone)dipalladium(0) (42.5 mg, 0.046 mmol), *tert*-butyl piperidine-4-carboxylate, hydrochloride (411 mg, 1.85 mmol), and 2-methyltetrahydrofuran (4.6 mL) were combined in a dry reaction vial under nitrogen, and then a 2 M solution of sodium *tert*-butoxide in THF (1.4 mL, 2.78 mmol) was added. The mixture was heated at 80 °C for 5 h. The reaction mixture was diluted with brine (200 mL) and extracted with ethyl acetate (2 × 200 mL). The combined organics were dried and concentrated under reduced pressure to give a brown gum which was purified by normal phase column chromatography (0-10% methanol in DCM). The appropriate samples were combined and dried under reduced pressure to afford the title product (243 mg, 0.418 mmol, 45% yield) as a brown gum. LCMS (HpH): R$_t$ = 1.18 min, [M+H]$^+$ 525.3, 96% purity. ^{1}H NMR: (400 MHz, methanol-d_4) δ ppm 7.98 - 8.01 (m, 1 H), 7.75 (dd, J = 2.5, 0.9 Hz, 1 H), 7.64 (d, J = 8.9 Hz, 1 H), 7.22 (d, J = 1.9 Hz, 1 H), 7.08 (dd, J = 9.1, 2.2 Hz, 1 H), 4.82 - 4.87 (m, 1 H), 4.04 (dd, J = 10.1, 9.1 Hz, 2 H), 3.80 (dd, J = 10.3, 4.4 Hz, 2 H), 3.65 (s, 3 H), 3.57 (br d, J = 12.3 Hz, 2 H), 3.25 (s, 6 H), 2.78 (td, J = 11.8, 2.4 Hz, 2 H), 2.33 - 2.41 (m, 1 H), 2.19 (s, 3 H), 2.01 (br dd, J = 13.3, 3.4 Hz, 2 H), 1.78 - 1.90 (m, 2 H), 1.47 (s, 9 H).

Methyl 4-(((1,3-dimethoxypropan-2-yl)amino)-3-nitrobenzoate (15)

Methyl 4-fluoro-3-nitrobenzoate (2.0 g, 10.04 mmol) and 1,3-dimethoxypropan-2-amine (1.55 g, 13.06 mmol) were dissolved in acetonitrile (13.4 mL), and potassium carbonate (2.08 g, 15.06 mmol) was added. The mixture was stirred at 80 °C for 8 h, then the mixture was allowed to cool down to rt. The mixture was diluted with water (100 mL) and extracted with ethyl acetate (2 × 100 mL). The organic layer was washed with water (100 mL) and brine (100 mL), dried, and concentrated under reduced pressure to afford the title product (3.034 g, 9.36 mmol, 93% yield) as a red solid. LCMS (HpH): R$_t$ = 1.13 min, [M+H]$^+$ 299.1, 100% purity. ^{1}H NMR: (400 MHz, DMSO-d_6) δ ppm 8.62 (d, J = 1.9 Hz, 1 H), 8.54 (d, J = 8.5 Hz, 1 H), 7.94 - 8.00 (m, 1 H), 7.28 (d, J = 9.3 Hz, 1 H), 4.22 (dt, J = 8.4, 5.2 Hz, 1 H), 3.83 (s, 3 H), 3.50 - 3.58 (m, 4 H), 3.31 (s, 6 H).

9

Methyl 1-(1,3-dimethoxypropan-2-yl)-2-(1,5-dimethyl-6-oxo-1,6-dihydropyridin-3-yl)-1*H*-benzo[*d*]imidazole-5-carboxylate (16)

Methyl 4-((1,3-dimethoxypropan-2-yl)amino)-3-nitrobenzoate (2.10 g, 6.48 mmol) was dissolved in ethanol (12 mL) with heating. 1,5-dimethyl-6-oxo-1,6-dihydropyridine-3-carbaldehyde (1.07 g, 7.12 mmol) was added to the suspension, followed by water (6.00 mL) and sodium dithionite (3.44 g, 16.1 mmol), and the mixture was heated at 90 °C for 18 h. The mixture was evaporated to approximately half its original volume, then diluted with water (200 mL), and extracted with ethyl acetate (200 mL) twice. The combined organics were washed with brine (200 mL), concentrated under reduced pressure and sonicated to afford the title product (1.79 g, 4.49 mmol, 69% yield) as a white solid. LCMS (HpH): R_t = 0.9 min, [M+H]+ 400.2, 100% purity. ^{1}H NMR: (400 MHz, DMSO-d_6) δ ppm 8.19 - 8.25 (m, 1 H), 8.09 (d, J = 2.4 Hz, 1 H), 7.90 - 7.96 (m, 1 H), 7.82 - 7.87 (m, 1 H), 7.66 - 7.71 (m, 1 H), 4.84 - 4.94 (m, 1 H), 4.02 - 4.07 (m, 2 H), 3.88 (s, 3 H), 3.78 (dd, J = 10.5, 4.6 Hz, 2 H), 3.55 (s, 3 H), 3.16 (s, 6 H), 2.10 (s, 3 H).

Tert-butyl (4-bromo-2-nitrophenyl)glycinate (17)

4-Bromo-1-fluoro-2-nitrobenzene (0.700 ml, 5.68 mmol) and *tert*-butyl glycinate (969 mg, 7.39 mmol) were dissolved in acetonitrile (7.6 mL), and potassium carbonate (1.17 g, 8.52 mmol) was added. The mixture was stirred at 80 °C for 8 h, then the mixture was allowed to cool down to rt. The mixture was diluted with water (100 mL) and extracted with ethyl acetate (2 × 100 mL). The organic layer was washed with brine (100 mL), dried, and concentrated under reduced pressure to afford the title product (2.09 g, 5.68 mmol, 100% yield) as a red solid. LCMS (HpH): R_t = 1.39 min, [M+H]+ not observed, 98% purity. ^{1}H NMR: (400 MHz, DMSO-d_6) δ ppm 8.37 (t, J = 5.6 Hz, 1 H), 8.15 - 8.22 (m, 1 H), 7.67 (dd, J = 8.8, 2.4 Hz, 1 H), 6.90 (d, J = 8.8 Hz, 1 H), 4.16 (d, J = 5.3 Hz, 2 H), 1.44 (s, 9 H).

Tert-butyl 2-(5-bromo-2-(1,5-dimethyl-6-oxo-1,6-dihydropyridin-3-yl)-1*H*-benzo[*d*]imidazol-1-yl)acetate (18)

Tert-butyl (4-bromo-2-nitrophenyl)glycinate (2.00 g, 6.04 mmol) was dissolved in ethanol (11.2 mL) with heating. 1,5-dimethyl-6-oxo-1,6-dihydropyridine-3-carbaldehyde (1.00 g, 6.64 mmol) was added to the suspension, followed by water (5.6 mL) and sodium dithionite (3.21 g, 15.1 mmol), and the mixture was heated at 90°C for 18 h. The reaction mixture was diluted in water (200 mL) and extracted with ethyl acetate (2 x 200 mL). The combined organics were washed with brine (100 mL) and concentrated under reduced pressure to afford the title product (1.25 g, 2.90 mmol, 48% yield) as a white solid. LCMS (HpH): R_t = 1.14 min, [M+H]+ 432.1, 90% purity. ^{1}H NMR: (400 MHz, DMSO-d_6) δ ppm 8.07 (d, J = 2.4 Hz, 1 H), 7.83 (d, J = 1.9 Hz, 1 H), 7.61 - 7.64 (m, 1 H), 7.58 (d, J = 8.3 Hz, 1 H), 7.42 (dd, J = 8.5, 1.7 Hz, 1 H), 5.20 (s, 2 H), 3.54 (s, 3 H), 2.08 (s, 3 H), 1.33 - 1.36 (m, 9 H).

Tert-butyl 2-(2-(1,5-dimethyl-6-oxo-1,6-dihydropyridin-3-yl)-5-morpholino-1*H*-benzo[*d*]imidazol-1-yl)acetate (19)

To a solution of *tert*-butyl 2-(5-bromo-2-(1,5-dimethyl-6-oxo-1,6-dihydropyridin-3-yl)-1*H*-benzo[*d*]imidazol-1-yl)acetate (100 mg, 0.231 mmol), RuPhos Pd G2 (17.9 mg, 0.023 mmol) and morpholine (65.7 μL, 0.694 mmol) in toluene (1.2 mL) was added cesium carbonate (226 mg, 0.694 mmol). The reaction vial was purged with nitrogen and stirred at 100 °C overnight. A second portion of RuPhos Pd G2 (17.97 mg, 0.023

mmol) was added and the reaction stirred for 72 h at 100 °C. The reaction mixture was purified by MDAP (HpH) to afford the title product (22 mg, 0.050 mmol, 22% yield) as a white solid. LCMS (HpH): R_t = 0.94 min, [M+H]+ 439.3, 98% purity. ^{1}H NMR: (400 MHz, DMSO-d_6) δ ppm 7.99 - 8.02 (m, 1 H), 7.60 - 7.62 (m, 1 H), 7.41 (d, J = 8.8 Hz, 1 H), 7.11 (d, J = 1.9 Hz, 1 H), 7.02 (dd, J = 8.8, 2.4 Hz, 1 H), 5.09 (s, 2 H), 3.72 - 3.80 (m, 4 H), 3.53 (s, 3 H), 3.05 - 3.12 (m, 4 H), 2.08 (s, 3 H), 1.35 (s, 9 H).

Large D2B library

Boc protected materials were all prepared according to standard sp²-sp³ cross coupling procedure: To RuPhos Pd G3 (30 mol%), aryl bromide **11** (1 eq.) and the relevant alkyl trifluoroborate (1.4 eq.) in toluene (9 parts) was added tripotassium phosphate (4 eq.). Water (1 part) was added and the reaction mixture purged with nitrogen then heated to 100 °C for 20 h. The reaction mixture was diluted with ethyl acetate and filtered then the solvent removed under a flow of nitrogen. The crude product was dissolved in 1:1 DMSO/methanol solution and purified by high pH MDAP. The relevant fractions were combined and concentrated *in vacuo* to give the products.

	R group	Yield	LCMS	^{1}H NMR
12.1	⟍⟍⟍NHBoc	20%	LCMS: (2 min high pH): t_R = 1.04 min, [M+H]+ 499.2 (96% purity).	^{1}H NMR: (400 MHz, CDCl₃) δ 7.88 (d, J = 2.4 Hz, 1H), 7.71 – 7.69 (m, 1H), 7.56 (d, J = 1.2 Hz, 1H), 7.42 (d, J = 8.3 Hz, 1H), 7.08 (dd, J = 8.3, 1.7 Hz, 1H), 4.82 (tt, J = 8.0, 5.0 Hz, 1H), 4.58 (br s, 1H), 3.94 (dd, J = 10.0, 8.1 Hz, 2H), 3.85 (dd, J = 10.0, 5.1 Hz, 2H), 3.62 (s, 3H), 3.28 (s, 6H), 3.18 (q, J = 6.5 Hz, 2H), 2.77 (t, J = 7.7 Hz, 2H), 2.22 (s, 3H), 1.91 – 1.83 (m, 2H), 1.45 (s, 9H).
12.2	⟍⟍⟍NHBoc	35%	LCMS: (2 min high pH): t_R = 0.99 min, [M+H]+ 485.2 (100% purity).	^{1}H NMR: (400 MHz, CDCl₃) δ 0.00 (d, J = 2.2 Hz, 1H), 7.68 (dd, J = 2.2, 1.2 Hz, 1H), 7.58 – 7.52 (m, 1H), 7.44 (d, J = 8.3 Hz, 1H), 7.07 (br d, J = 8.1 Hz, 1H), 4.86 – 4.75 (m, 1H), 4.67 (br s, 1H), 3.98 – 3.89 (m, 2H), 3.86 – 3.78 (m, 2H), 3.59 (s, 3H), 3.45 – 3.35 (m, 2H), 3.32 – 3.21 (m, 6H), 2.89 (br t, J = 7.0 Hz, 2H), 2.19 (s, 3H), 1.40 (s, 9H).
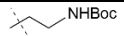
10

#	Structure	Yield	LCMS	¹H NMR
12.3	[structure: N-Boc piperidine]	51%	LCMS: (2 min high pH): t_R = 1.20 min, $[M+H]^+$ 539.2 (98% purity).	¹H NMR: (400 MHz, CDCl₃) δ 7.87 – 7.81 (m, 1H), 7.70 – 7.63 (m, 1H), 7.51 – 7.46 (m, 1H), 7.42 – 7.36 (m, 1H), 7.02 – 6.95 (m, 1H), 4.84 – 4.74 (m, 1H), 4.11 – 3.97 (m, 2H), 3.96 – 3.87 (m, 2H), 3.85 – 3.77 (m, 2H), 3.62 – 3.55 (m, 3H), 3.29 – 3.21 (m, 6H), 2.68 – 2.56 (m, 4H), 2.17 (s, 3H), 1.73 – 1.56 (m, 3H), 1.46 – 1.37 (m, 9H), 1.23 – 1.07 (m, 2H)
12.4	[structure: N-Boc piperidine with ether]	46%	LCMS: (2 min high pH): t_R = 1.11 min, $[M+H]^+$ 569.2 (100% purity).	¹H NMR: (400 MHz, CDCl₃) δ 7.85 (d, *J* = 2.4 Hz, 1H), 7.69 – 7.66 (m, 2H), 7.47 (d, *J* = 8.3 Hz, 1H), 7.21 (dd, *J* = 8.4, 1.6 Hz, 1H), 4.85 – 4.77 (m, 1H), 4.58 (s, 2H), 4.11 – 4.00 (m, 2H), 3.92 (dd, *J* = 9.8, 8.2 Hz, 2H), 3.81 (dd, *J* = 9.8, 4.9 Hz, 2H), 3.58 (s, 3H), 3.31 (d, *J* = 6.1 Hz, 2H), 3.24 (s, 6H), 2.66 (br t, *J* = 12.2 Hz, 2H), 2.18 (s, 3H), 1.81 – 1.67 (m, 3H), 1.41 (s, 9H), 1.12 (qd, *J* = 12.3, 4.3 Hz, 2H)
12.5	[structure: N-Boc piperidine]	18%	LCMS: (2 min high pH): t_R = 1.20 min, $[M+H]^+$ 539.2 (88% purity). Note: 12% carbazole from RuPhos Pd G3.	¹H NMR: (400 MHz, CDCl₃) δ 7.87 (d, *J* = 2.4 Hz, 1H), 7.70 (dd, *J* = 2.4, 1.2 Hz, 1H), 7.52 (d, *J* = 1.2 Hz, 1H), 7.41 (d, *J* = 8.3 Hz, 1H), 7.04 (dd, *J* = 8.4, 1.6 Hz, 1H), 4.85 – 4.77 (m, 1H), 3.96 – 3.82 (m, 6H), 3.60 (s, 3H), 3.27 (d, *J* = 2.0 Hz, 6H), 2.83 – 2.73 (m, 1H), 2.73 – 2.66 (m, 1H), 2.61 – 2.47 (m, 2H), 2.21 (s, 3H), 1.83 – 1.74 (m, 2H), 1.67 – 1.58 (m, 1H), 1.41 (s, 10H), 1.21 – 1.10 (m, 1H)
12.6	[structure: N-Boc piperazine]	27%	LCMS: (2 min high pH): t_R = 1.05 min, $[M+H]^+$ 540.2 (100% purity).	¹H NMR: (400 MHz, CDCl₃) δ 7.88 (d, *J* = 2.2 Hz, 1H), 7.70 (dd, *J* = 2.2, 1.2 Hz, 1H), 7.67 (br s, 1H), 7.46 (d, *J* = 8.3 Hz, 1H), 7.23 (dd, *J* = 8.3, 1.5 Hz, 1H), 4.87 – 4.78 (m, 1H), 3.94 (dd, *J* = 9.8, 8.1 Hz, 2H), 3.84 (dd, *J* = 9.8, 4.9 Hz, 2H), 3.62 (s, 2H), 3.61 (s, 3H), 3.44 – 3.39 (m, 4H), 3.27 (s, 6H), 2.42 (br t, *J* = 4.9 Hz, 4H), 2.20 (s, 3H), 1.44 (s, 9H).
12.7	[structure: N-Boc azetidine]	41%	LCMS: (2 min high pH): t_R = 1.08 min, $[M+H]^+$ 511.2 (87% purity).	¹H NMR: (400 MHz, CDCl₃) δ 7.85 (d, *J* = 2.4 Hz, 1H), 7.71 – 7.66 (m, 1H), 7.50 (s, 1H), 7.42 (d, *J* = 8.3 Hz, 1H), 7.02 (dd, *J* = 8.3, 1.7 Hz, 1H), 4.86 – 4.75 (m, 1H), 3.98 (t, *J* = 8.3 Hz, 2H), 3.92 (dd, *J* = 9.8, 8.1 Hz, 2H), 3.82 (dd, *J* = 9.8, 4.9 Hz, 2H), 3.67 (dd, *J* = 8.8, 5.4 Hz, 2H), 3.58 (s, 3H), 3.25 (s, 6H), 3.00 (d, *J* = 7.8 Hz, 2H), 2.92 – 2.79 (m, 1H), 2.19 (s, 3H), 1.41 (s, 9H)
12.8	[structure: NHBoc cyclobutane]	58%	LCMS: (2 min high pH): t_R = 1.11 min, $[M+H]^+$ 525.2 (84% purity).	¹H NMR: (400 MHz, CDCl₃) δ 8.80 (br s, 1H), 7.90 (d, *J* = 2.4 Hz, 1H), 7.66 (s, 1H), 7.49 (d, *J* = 8.3 Hz, 1H), 7.40 (d, *J* = 8.3 Hz, 1H), 7.05 – 6.96 (m, 1H), 5.01 – 4.82 (m, 1H), 4.81 – 4.74 (m, 1H), 3.91 (dd, *J* = 9.8, 8.3 Hz, 2H), 3.79 (dd, *J* = 10.3, 4.9 Hz, 2H), 3.57 (s, 3H), 3.22 (s, 6H), 2.84 (d, *J* = 8.3 Hz, 1H), 2.75 (d, *J* = 7.2 Hz, 1H), 2.56 – 2.36 (m, 2H), 2.24 – 2.09 (m, 5H), 2.00 – 1.89 (m, 1H), 1.58 – 1.47 (m, 1H), 1.42 – 1.35 (m, 9H). Note: residual formic acid present

All intermediates were subjected to Boc-deprotection using TFA (5 eq.) in DCM at room temperature until reaction was complete. Reaction mixtures were concentrated under a stream of nitrogen to give the amine products as TFA salts in quantitative yield.

#	R group	LCMS	¹H NMR
13.1	[structure: propyl NH₂]	LCMS: (2 min high pH): t_R = 0.83 min, $[M+H]^+$ 399.2 (92% purity).	Consistent with structure. See ELN85695 for full data write up
13.2	[structure: ethyl NH₂]	LCMS: (2 min high pH): t_R = 0.77 min, $[M+H]^+$ 385.2 (100% purity).	¹H NMR: (400 MHz, CDCl₃) δ 8.55 (br s, 3H), 8.40 (br s, 1H), 0.00 (d, *J* = 8.6 Hz, 1H), 7.69 – 7.60 (m, 2H), 7.34 (d, *J* = 8.6 Hz, 1H), 4.89 (tt, *J* = 8.2, 4.2 Hz, 1H), 4.01 (dd, *J* = 10.1, 8.4 Hz, 2H), 3.84 (dd, *J* = 10.1, 4.2 Hz, 2H), 3.65 (s, 3H), 3.34 (br s, 2H), 3.29 (s, 6H), 3.18 – 3.10 (m, 2H), 2.21 (s, 3H).
13.3	[structure: piperidine NH]	LCMS: (2 min high pH): t_R = 0.94 min, $[M+H]^+$ 439.2 (98% purity).	¹H NMR: (400 MHz, CDCl₃) δ 9.39 (br d, *J* = 5.4 Hz, 1H), 9.04 (br d, *J* = 5.4 Hz, 1H), 8.31 (s, 1H), 7.73 – 7.68 (m, 3H), 7.30 – 7.26 (m, 1H), 5.00 – 4.90 (m, 1H), 4.08 – 4.01 (m, 2H), 3.84 (dd, *J* = 10.3, 3.9 Hz, 2H), 3.65 (s, 3H), 3.39 (br d, *J* = 10.6 Hz, 2H), 3.30 (s, 6H), 2.93 –

11

			2.79 (m, 2H), 2.77 (br d, *J* = 6.6 Hz, 2H), 2.21 (s, 3H), 1.95 – 1.85 (m, 1H), 1.82 (br d, *J* = 14.3 Hz, 2H), 1.68 – 1.55 (m, 2H)
13.4		LCMS: (2 min high pH): t_R = 0.94 min, [M+H]⁺ 469.2 (100% purity).	¹H NMR: (400 MHz, CDCl₃) δ 9.56 (br s, 1H), 8.99 (br s, 1H), 8.30 (br s, 1H), 8.03 (br s, 1H), 7.79 – 7.69 (m, 2H), 7.45 – 7.39 (m, 1H), 5.03 – 4.89 (m, 1H), 4.65 (s, 2H), 4.12 – 4.02 (m, 2H), 3.89 – 3.80 (m, 2H), 3.64 (br s, 3H), 3.54 – 3.36 (m, 4H), 3.32 – 3.25 (m, 6H), 3.05 – 2.87 (m, 2H), 2.20 (s, 3H), 1.99 – 1.87 (m, 3H), 1.85 – 1.69 (m, 2H)
13.5		LCMS: (2 min high pH): t_R = 0.96 min, [M+H]⁺ 439.2 (94% purity).	¹H NMR (400 MHz, CDCl₃) δ 9.56 – 9.44 (m, 1H), 9.16 – 9.01 (m, 1H), 8.30 (s, 1H), 7.80 – 7.67 (m, 3H), 7.33 – 7.28 (m, 1H), 4.95 (tt, *J* = 8.6, 4.2 Hz, 1H), 4.05 (dd, *J* = 10.1, 9.1 Hz, 2H), 3.84 (dd, *J* = 10.1, 3.9 Hz, 2H), 3.65 (s, 3H), 3.38 – 3.25 (m, 8H), 2.90 – 2.77 (m, 1H), 2.74 (br d, *J* = 6.9 Hz, 2H), 2.69 – 2.56 (m, 1H), 2.34 – 2.23 (m, 1H), 2.21 (s, 3H), 1.92 – 1.76 (m, 3H), 1.28 – 1.22 (m, 1H)
13.6		LCMS: (2 min high pH): t_R = 0.79 min, [M+H]⁺ 440.2 (89% purity).	¹H NMR (400 MHz, CDCl₃) δ 8.21 (br d, *J* = 2.0 Hz, 1H), 8.02 (br s, 1H), 7.82 (d, *J* = 8.6 Hz, 1H), 7.70 – 7.64 (m, 1H), 7.57 (d, *J* = 8.6 Hz, 1H), 4.95 (tt, *J* = 8.4, 4.1 Hz, 1H), 4.34 – 4.20 (m, 2H), 4.09 – 4.00 (m, 2H), 3.84 (dd, *J* = 10.3, 3.9 Hz, 2H), 3.67 – 3.60 (m, 3H), 3.55 – 3.44 (m, 4H), 3.42 – 3.33 (m, 4H), 3.30 (s, 6H), 2.20 (s, 3H). Note: N-H not visible
13.7		LCMS: (2 min high pH): t_R = 0.83 min, [M+H]⁺ 441.2 (100% purity).	¹H NMR (400 MHz, CDCl₃) δ 9.89 (br s, 2H), 8.26 (s, 1H), 7.86 – 7.66 (m, 3H), 7.40 – 7.29 (m, 1H), 5.05 – 4.83 (m, 1H), 4.36 – 3.79 (m, 9H), 3.66 (s, 3H), 3.29 (s, 6H), 3.16 (br s, 2H), 2.21 (s, 3H)
13.8		LCMS: (2 min high pH): t_R = 0.88 min, [M+H]⁺ 425.2 (95% purity).	¹H NMR (400 MHz, CDCl₃) δ 8.52 – 8.32 (m, 3H), 8.28 – 8.21 (m, 1H), 7.73 – 7.61 (m, 3H), 7.31 – 7.23 (m, 1H), 5.00 – 4.90 (m, 1H), 4.10 – 4.01 (m, 2H), 3.98 (s, 1H), 3.89 – 3.82 (m, 2H), 3.62 (s, 3H), 3.34 – 3.26 (m, 6H), 2.91 – 2.74 (m, 3H), 2.41 – 2.29 (m, 2H), 2.20 – 2.07 (m, 4H), 2.06 – 1.94 (m, 1H)

Amines were dissolved in methanol and passed through an SCX cartridge, eluting with 4 M ammonia in methanol, then concentrating under a stream of nitrogen to give the free amine which was made up to a 0.1 M stock solution in DMSO for D2B amide coupling reaction with library of E3 ligase-linker intermediates.

Synthesis of purified PROTACs

HER2 PROTACs

(2*S*,4*R*)-1-((*S*)-2-(2-(2-(2-(4-(4-((3-Chloro-4-((3-fluorobenzyl)oxy)phenyl)amino) quinazolin-6-yl)phenoxy)ethoxy)ethoxy)acetamido)-3,3-dimethylbutanoyl)-4-hydroxy-*N*-((*S*)-1-(4-(4-methylthiazol-5-yl)phenyl)ethyl)pyrrolidine-2-carboxamide (3)

A solution of *tert*-butyl 2-(2-(2-(4-(4-((3-chloro-4-((3-fluorobenzyl)oxy)phenyl)amino) quinazolin-6-yl)phenoxy)ethoxy)ethoxy)acetate (40 mg, 0.059 mmol) in a mixture of TFA (1 mL) and DCM (0.5 mL) was stirred for 2h. The solvent was removed under reduced pressure and the crude product was used in the next step without further purification. To a solution of the crude material and (2*S*,4*R*)-1-((*S*)-2-amino-3,3-dimethylbutanoyl)-4-hydroxy-*N*-((*S*)-1-(4-(4-methylthiazol-5-yl)phenyl)ethyl)pyrrolidine-2-carboxamide (79 mg, 0.178 mmol) in DMF (1.2 mL) was added HATU (45.1 mg, 0.119 mmol) and DIPEA (51.8 μL, 0.297 mmol) and the resulting mixture was stirred overnight at room temperature. The reaction mixture was diluted up in ethyl acetate (40 mL) and washed with 5% LiCl aqueous solution (4 x 40 mL), the organic phase was passed through a hydrophobic frit and concentrated under reduced pressure. The crude was purified by MDAP (HpH) to afford the title product (33 mg, 0.032 mmol, 53% yield) as a brown gum. LCMS (HpH): R_t = 1.43 min, [M+H]⁺ 1044.2, 100% purity. ¹H NMR: (400 MHz, DMSO-*d₆*) δ ppm 9.85 (s, 1 H), 8.96 (s, 1 H), 8.75 (d, *J* = 1.9 Hz, 1 H), 8.57 (s, 1 H), 8.40 (d, *J* = 7.8 Hz, 1 H), 8.16 (dd, *J* = 8.8, 1.9 Hz, 1 H), 8.02 (d, *J* = 2.4 Hz, 1 H), 7.78 - 7.83 (m, 3 H), 7.74 - 7.78 (m, 1 H), 7.27 - 7.51 (m, 9 H), 7.16 - 7.22 (m, 1 H), 7.11 - 7.15 (m, 2 H), 5.26 (s, 2 H), 5.12 (d, *J* = 3.9 Hz, 1 H), 4.90 (s, 1 H), 4.57 (d, *J* = 9.3 Hz, 1 H), 4.46 (t, *J* = 8.1 Hz, 1 H), 4.29 (br s, 1 H), 4.22 (t, *J* = 4.6 Hz, 2 H), 3.99 - 4.01 (m, 2 H), 3.81 - 3.87 (m, 2 H), 3.65 - 3.71 (m, 4 H), 3.54 - 3.65 (m, 2 H), 2.41 - 2.45 (m, 3 H), 2.00 - 2.11 (m, 1 H), 1.78 (ddd, *J* = 12.9, 8.7, 4.4 Hz, 1 H), 1.33 (d, *J* = 6.8 Hz, 3 H), 0.95 (s, 9 H).

(2*R*,4*S*)-1-((*R*)-2-(2-(2-(2-(4-(4-((3-Chloro-4-((3-fluorobenzyl)oxy)phenyl)amino) quinazolin-6-yl)phenoxy)ethoxy)ethoxy)acetamido)-3,3-dimethylbutanoyl)-4-hydroxy-*N*-((*R*)-1-(4-(4-methylthiazol-5-yl)phenyl)ethyl)pyrrolidine-2-carboxamide (4)

A solution of *tert*-butyl 2-(2-(2-(4-(4-((3-chloro-4-((3-fluorobenzyl)oxy)phenyl)amino) quinazolin-6-yl)phenoxy)ethoxy)ethoxy)acetate (50 mg, 0.074 mmol) in a mixture of TFA (2 mL) and DCM (1 mL) was stirred for 2 h. The solvent was removed under reduced pressure and the crude product was used in the next step without further purification. To a solution of the crude material and (2*R*,4*S*)-1-((*R*)-2-amino-3,3-dimethylbutanoyl)-4-hydroxy-*N*-((*S*)-1-(4-(4-methylthiazol-5-yl)phenyl)ethyl)pyrrolidine-2-carboxamide (66 mg, 0.148 mmol) in DMF (1 mL) was added HATU (56.4 mg, 0.148 mmol) and DIPEA (65.0 μL, 0.371 mmol) and the resulting mixture was stirred overnight at room temperature. The reaction mixture was diluted in ethyl acetate (40 mL) and washed with 5% LiCl aqueous solution (4 x 40 mL), the organic phase was passed through a hydrophobic frit and concentrated under reduced pressure. The crude was purified by MDAP (HpH) to afford the title product (51 mg, 0.049 mmol, 66% yield) as a brown gum. LCMS (HpH): R_t = 1.43 min, MH⁺ 1044, 100% purity. ¹H NMR: (400 MHz, DMSO-*d₆*) δ ppm 9.86 - 9.89 (m, 1 H), 8.96 (s, 1 H), 8.75 (d, *J* = 1.4 Hz, 1 H), 8.57 (s, 1 H), 8.40 (d, *J* = 7.8 Hz, 1 H), 8.16 (dd, *J* = 8.8, 1.9 Hz, 1 H), 8.02 (d, *J* = 2.4 Hz, 1 H), 7.80 - 7.87 (m, 3 H), 7.76 (dd, *J* = 8.8, 2.4 Hz, 1 H), 7.41 - 7.51

12

 ORCID: https://orcid.org/0009-0006-8159-9423

(m, 2 H), 7.37 - 7.40 (m, 2 H), 7.27 - 7.35 (m, 5 H), 7.18 - 7.22 (m, 1 H), 7.12 - 7.15 (m, 2 H), 5.26 (s, 2 H), 5.12 (d, J = 3.4 Hz, 1 H), 4.90 (t, J = 7.3 Hz, 1 H), 4.57 (d, J = 9.8 Hz, 1 H), 4.46 (t, J = 8.1 Hz, 1 H), 4.29 (br s, 1 H), 4.22 (t, J = 4.6 Hz, 2 H), 4.00 (s, 1 H), 3.80 - 3.87 (m, 2 H), 3.57 - 3.73 (m, 6 H), 2.43 (s, 3 H), 2.02 - 2.10 (m, 1 H), 1.78 (ddd, J = 13.0, 8.6, 4.9 Hz, 1 H), 1.33 (d, J = 7.3 Hz, 3 H), 0.95 (s, 9 H).

(2*S*,4*R*)-1-((*S*)-2-(2-(2-(2-(4-(4-((3-chloro-4-((3-fluoro-benzyl)oxy)phenyl)amino) quinazolin-6-yl)phenoxy)acet-amido)ethoxy)acetamido)-3,3-dimethylbutanoyl)-4-hy-droxy-*N*-((*S*)-1-(4-(4-methylthiazol-5-yl)phenyl)ethyl) pyrrolidine-2-carboxamide (6.2)

A solution of 2-(4-(4-((3-chloro-4-((3-fluorobenzyl)oxy) phenyl)amino)quinazolin-6-yl)phenoxy) acetic acid (60.0 mg, 0.113 mmol), (2*S*,4*R*)-1-((*S*)-2-(2-(2-(2-aminoethoxy)acetam-ido)-3,3-dimethylbutanoyl)-4-hydroxy-*N*-((*S*)-1-(4-(4-methyl-thiazol-5-yl)phenyl)ethyl)pyrrolidine-2-carboxamide (3.53) (74.0 mg, 0.136 mmol), EDC. HCl (32.6 mg, 0.170 mmol), Oxy-maPure (32 mg, 0.226 mmol) and NMM (100 μL, 0.906 mmol) in DMF (1.1 mL) was stirred at room temperature for 5 h. The reaction mixture was purified by MDAP (HpH) to afford the ti-tle product (71 mg, 0.060 mmol, 53% yield) as a white solid. LCMS (HpH): R_t = 1.35 min, [M+2H]$^{2+}$ 529.5, 98% purity. ^{1}H NMR: (400 MHz, DMSO-d_6) δ ppm 9.84 - 9.90 (m, 1 H), 8.97 (s, 1 H), 8.75 (d, J = 1.4 Hz, 1 H), 8.58 (s, 1 H), 8.40 (d, J = 7.8 Hz, 1 H), 8.27 (s, 1 H), 8.16 (dd, J = 8.8, 1.9 Hz, 1 H), 8.02 (d, J = 2.4 Hz, 1 H), 7.81 - 7.89 (m, 3 H), 7.77 (dd, J = 9.0, 2.6 Hz, 1 H), 7.38 - 7.51 (m, 4 H), 7.27 - 7.36 (m, 5 H), 7.16 (d, J = 8.8 Hz, 3 H), 5.26 (s, 2 H), 5.12 (d, J = 3.4 Hz, 1 H), 4.89 (t, J = 7.0 Hz, 1 H), 4.61 (s, 2 H), 4.57 (d, J = 9.2 Hz, 1 H), 4.46 (t, J = 8.0 Hz, 1 H), 4.29 (br s, 1 H), 3.98 (d, J = 5.8 Hz, 2 H), 3.59 (dt, J = 9.5, 5.0 Hz, 4 H), 3.34 - 3.44 (m, 2 H), 2.44 (s, 3 H), 1.98 - 2.10 (m, 1 H), 1.78 (s, 1 H), 1.34 (d, J = 6.8 Hz, 3 H), 0.95 (s, 9 H).

(2*S*,4*R*)-1-((*S*)-2-(*Tert*-butyl)-14-(4-(4-((3-chloro-4-((3-fluorobenzyl)oxy)phenyl)amino) quinazolin-6-yl)phe-noxy)-4,13-dioxo-6,9-dioxa-3,12-diazatetradecanoyl)-4-hydroxy-*N*-((*S*)-1-(4-(4-methylthiazol-5-yl)phenyl)ethyl) pyrrolidine-2-carboxamide (6.7)

A solution of 2-(4-(4-((3-chloro-4-((3-fluoroben-zyl)oxy)phenyl)amino)quinazolin-6-yl)phenoxy)acetic acid (60 mg, 0.113 mmol), (2*S*,4*R*)-1-((*S*)-2-(2-(2-(2-aminoeth-oxy)ethoxy)acetamido)-3,3-dimethylbutanoyl)-4-hydroxy-*N*-((*S*)-1-(4-(4-methylthiazol-5-yl)phenyl)ethyl)pyrrolidine-2-carboxamide (66.8 mg, 0.113 mmol), EDC.HCl (32.6 mg, 0.170 mmol), OxymaPure (32 mg, 0.226 mmol) and NMM (92 mg, 0.906 mmol) in DMF (1.1 mL) was stirred at room temperature for 5 h. The reaction mixture was purified by MDAP (HpH) to afford the title product (98 mg, 0.080 mmol, 71% yield) as a white solid. LCMS (Formic): R_t = 1.25 min, [M+2H]$^{2+}$ 551.5, 99% purity. ^{1}H NMR: (400 MHz, DMSO-d_6) δ ppm 9.87 (s, 1 H), 8.96 (s, 1 H), 8.74 (d, J = 1.4 Hz, 1 H), 8.57 (s, 1 H), 8.40 (d, J = 7.8 Hz, 1 H), 8.12 - 8.19 (m, 2 H), 8.02 (d, J = 2.9 Hz, 1 H), 7.80 - 7.88 (m, 3 H), 7.76 (dd, J = 9.05, 2.6 Hz, 1 H), 7.47 (td, J = 7.9, 6.1 Hz, 1 H), 7.38 - 7.43 (m, 3 H), 7.27 - 7.36 (m, 5 H), 7.11 - 7.21 (m, 3 H), 5.26 (s, 2 H), 5.13 (d, J = 3.4 Hz, 1 H), 4.89 (t, J = 7.3 Hz, 1 H), 4.53 - 4.62 (m, 3 H), 4.46 (t, J = 8.0 Hz, 1 H), 4.29 (br s, 1 H), 3.97 (s, 2 H), 3.55 - 3.66 (m, 6 H), 3.49 - 3.54 (m, 2 H), 3.33 - 3.41 (m, 2 H), 2.44 (s, 3 H), 2.06 (br dd, J = 12.2, 8.3 Hz, 1 H), 1.78 (ddd, J = 12.8, 8.6, 4.4 Hz, 1 H), 1.35 (d, J = 6.8 Hz, 3 H), 0.90 - 0.98 (m, 9 H).

BRD4 PROTACs

1-(1-(1,3-Dimethoxypropan-2-yl)-2-(1,5-dimethyl-6-oxo-1,6-dihydropyridin-3-yl)-1*H*-benzo[*d*]imidazol-5-yl)-*N*-(12-((2-(2,6-dioxopiperidin-3-yl)-1-oxoisoindolin-4-yl)amino)-12-oxododecyl)piperidine-4-carboxamide (8.36)

To a solution of 1-(1-(1,3-dimethoxypropan-2-yl)-2-(1,5-di-methyl-6-oxo-1,6-dihydropyridin-3-yl)-1*H*-benzo[*d*]imidazol-5-yl)piperidine-4-carboxylic acid (50.0 mg, 0.107 mmol), 12-amino-*N*-(2-(2,6-dioxopiperidin-3-yl)-1-oxoisoindolin-4-yl)dodecanamide, hydrochloride (63.1 mg, 0.128 mmol) and HATU (101 mg, 0.267 mmol) in DMF (534 μL) was added DIPEA (55.9 μL, 0.320 mmol) and the reaction was stirred at room temperature for 3 h. The reaction was purified directly by MDAP (HpH) to afford the title product (38 mg, 0.041 mmol, 38% yield) as a white solid. LCMS (HpH): R_t = 1.07 min, [M+H]$^+$ 907.5, 98% purity. ^{1}H NMR: (400 MHz, DMSO-d_6) δ ppm 9.74 (s, 1 H), 7.97 - 8.00 (m, 1 H), 7.81 (dd, J = 6.8, 1.9 Hz, 1 H), 7.73 (t, J = 5.3 Hz, 1 H), 7.64 (dd, J = 2.4, 0.9 Hz, 1 H), 7.59 (d, J = 8.8 Hz, 1 H), 7.49 (d, J = 1.9 Hz, 1 H), 7.45 - 7.51 (m, 1 H), 7.09 (d, J = 1.9 Hz, 1 H), 6.94 (dd, J = 8.8, 2.4 Hz, 1 H), 5.14 (dd, J = 13.2, 4.8 Hz, 1 H), 4.76 (dt, J = 8.8, 4.4 Hz, 1 H), 4.28 - 4.44 (m, 2 H), 3.96 (dd, J = 10.2, 8.8 Hz, 2 H), 3.74 (dd, J = 10.5, 4.6 Hz, 2 H), 3.61 (br d, J = 12.2 Hz, 2 H), 3.53 (s, 3 H), 3.16 (s, 6 H), 3.03 (br d, J = 6.3 Hz, 2 H), 2.92 (ddd, J = 17.3, 13.4, 5.3 Hz, 1 H), 2.55 - 2.69 (m, 3 H), 2.35 (br t, J = 7.5 Hz, 3 H), 2.17 - 2.30 (m, 1 H), 2.08 (s, 3 H), 1.99 - 2.06 (m, 1 H), 1.70 - 1.79 (m, 4 H), 1.56 - 1.65 (m, 2 H), 1.35 - 1.43 (m, 2 H), 1.22 - 1.34 (m, 14 H).

1-(1,3-Dimethoxypropan-2-yl)-2-(1,5-dimethyl-6-oxo-1,6-dihydropyridin-3-yl)-*N*-((*S*)-13-((2*S*,4*R*)-4-hydroxy-2-(((*S*)-1-(4-(4-methylthiazol-5-yl)phenyl)ethyl)carbamoyl) pyrrolidine-1-carbonyl)-14,14-dimethyl-11-oxo-3,6,9-tri-oxa-12-azapentadecyl)-1*H*-benzo[*d*]imidazole-5-carbox-amide (9.46)

To a solution of 1-(1,3-dimethoxypropan-2-yl)-2-(1,5-dime-thyl-6-oxo-1,6-dihydropyridin-3-yl)-1*H*-benzo[*d*]imidazole-5-carboxylic acid (50 mg, 0.130 mmol), (2*S*,4*R*)-1-((*S*)-14-amino-2-(*tert*-butyl)-4-oxo-6,9,12-trioxa-3-azatetradecanoyl)-4-hy-droxy-*N*-((*S*)-1-(4-(4-methylthiazol-5-yl)phenyl)ethyl)pyrroli-dine-2-carboxamide, hydrochloride (104 mg, 0.156 mmol) and HATU (123 mg, 0.324 mmol) in DMF (649 μL) was added DIPEA (68.0 μL, 0.389 mmol) and the reaction was stirred at room temperature for 3 h. The reaction was purified directly by MDAP (HpH) to afford the title product (56 mg, 0.055 mmol, 42% yield). LCMS (HpH): R_t = 0.96 min, [M+2H]$^{2+}$ 501.4, 98% purity. ^{1}H NMR: (400 MHz, DMSO-d_6) δ ppm 8.97 (s, 1 H), 8.50 (t, J = 5.6 Hz, 1 H), 8.39 - 8.44 (m, 1 H), 8.17 (d, J = 1.4 Hz, 1 H), 8.07 (d, J = 1.9 Hz, 1 H), 7.85 (d, J = 8.3 Hz, 1 H), 7.76 (dd, J = 8.5, 1.7 Hz, 1 H), 7.67 - 7.70 (m, 1 H), 7.40 - 7.46 (m, 2 H), 7.33 - 7.39 (m, 3 H), 5.13 (br s, 1 H), 4.82 - 4.94 (m, 2 H), 4.55 (d, J = 9.7 Hz, 1 H), 4.45 (s, 1 H), 4.29 (br s, 1 H), 4.02 (t, J = 9.5 Hz, 2 H), 3.95 (s, 2 H), 3.77 (dd, J = 10.5, 4.6 Hz, 2 H), 3.56 - 3.62 (m, 11 H), 3.54 (s, 3 H), 3.46 (br d, J = 5.8 Hz, 2 H), 3.15 (s, 6 H), 2.45 (s, 3 H), 2.09 (s, 3 H), 2.03 (br d, J = 8.8 Hz, 1 H), 1.73 - 1.83 (m, 1 H), 1.53 (s, 1 H), 1.34 - 1.40 (m, 1 H), 0.94 (s, 9 H).

(2*S*,4*R*)-*N*-(2-(2-(2-(2-(4-((1-(1,3-Dimethoxypropan-2-yl)-2-(1,5-dimethyl-6-oxo-1,6-dihy dropyridin-3-yl)-1*H*-benzo[*d*]imidazol-5-yl)methyl)piperidin-1-yl)-2-oxoeth-oxy)ethoxy) ethoxy)-4-(4-methylthiazol-5-yl)benzyl)-1-((*S*)-2-(1-fluorocyclopropane-1-carboxamido)-3,3-dime-thylbutanoyl)-4-hydroxypyrrolidine-2-carboxamide (20)

To a solution of 2-(2-(2-(2-(((2*S*,4*R*)-1-((*S*)-2-(1-fluorocy-clopropane-1-carboxamido)-3,3-dimethylbutanoyl)-4-

hydroxypyrrolidine-2-carboxamido)methyl)-5-(4-methylthia-zol-5-yl)phenoxy)ethoxy)ethoxy)acetic acid (36.0 mg, 53.05 µmol) in DMF (442.1 µL) was added HATU (20.2 mg, 53.05 µmol) and DIPEA (23.1 µL, 132.62 µmol), followed by 5-(1-(1,3-dimethoxypropan-2-yl)-5-(piperidin-4-ylmethyl)-1*H*-benzo[*d*]imidazol-2-yl)-1,3-dimethylpyridin-2(1*H*)-one, hydrochlo-ride (21 mg, 44.21 µmol) and the reaction mixture was stirred at room temperature for 22 h. The reaction mixture was diluted with 0.5 mL of DMF and purified by high pH MDAP to afford the title product (24 mg, 21 µmol, 48% yield) as a white solid. LCMS (HpH): R_t = 1.05 min, $[M+H]^+$ 1099.6, 100% purity. ^{1}H NMR: (CDCl$_3$, 400 MHz) δ 8.67 (s, 1H), 7.88 (d, 1H, *J* = 2.6 Hz), 7.71 - 7.68 (m, 1H), 7.51 (s, 1H), 7.43 (d, 1H, *J* = 8.3 Hz), 7.38 - 7.32 (m, 2H), 7.08 (dd, 1H, *J* = 9.1, 3.4 Hz), 7.03 - 6.95 (m, 2H), 6.91 - 6.89 (m, 1H), 4.87 - 4.79 (m, 1H), 4.68 - 4.61 (m, 1H), 4.59 (d, 1H, *J* = 9.1 Hz), 4.54 - 4.45 (m, 4H), 4.28 - 4.16 (m, 4H), 3.99 - 3.88 (m, 5H), 3.85 (dd, 2H, *J* = 9.8, 4.9 Hz), 3.82 - 3.71 (m, 5H), 3.70 - 3.64 (m, 1H), 3.62 (s, 3H), 3.29 (s, 6H), 2.97 - 2.87 (m, 1H), 2.69 - 2.63 (m, 2H), 2.52 (s, 4H), 2.37 - 2.25 (m, 1H), 2.22 (s, 3H), 2.15 (br dd, 1H, *J* = 13.3, 8.2 Hz), 1.88 - 1.78 (m, 2H), 1.73 (br d, 2H, *J* = 13.9 Hz), 1.36 - 1.14 (m, 6H), 0.98 (s, 9H).

Three other hits synthesised (**21**, **22** and **23**); structures not disclosed. Included for comparison of D2B and purified data, see Figure 6.

Standard amide coupling procedure

To a solution of carboxylic acid (10 mg, 1 eq.) in DMSO (0.3 mL) was added amine (1.5 eq.), EDC.HCl (1.5 eq.), OxymaPure (2 eq.), and NMM (8 eq). The reaction mixture was stirred at room temperature for 18 h. The reaction mixtures were di-rectly purified by high pH MDAP to obtain the desired PROTAC products.

1-(1-(1,3-Dimethoxypropan-2-yl)-2-(1,5-dimethyl-6-oxo-1,6-dihydropyridin-3-yl)-1*H*-benzo[*d*]imidazol-5-yl)-*N*-(6-(((*S*)-1-((2*S*,4*R*)-4-hydroxy-2-(((*S*)-1-(4-(4-methyl-thiazol-5-yl)phenyl)ethyl)carbamoyl)pyrrolidin-1-yl)-3,3-dimethyl-1-oxobutan-2-yl)amino)-6-oxohexyl)piperi-dine-4-carboxamide (8.8)

LCMS (Formic): R_t = 0.76 min, $[M+2H]^{2+}$ 505.1, 100% purity. ^{1}H NMR: (600 MHz, DMSO-d_6) δ 8.98 (s, 1H), 8.36 (d, *J* = 7.7 Hz, 1H), 7.99 (s, 1H), 7.80 - 7.73 (m, 2H), 7.64 (s, 1H), 7.60 (d, *J* = 8.8 Hz, 1H), 7.43 (d, *J* = 7.7 Hz, 2H), 7.38 (d, *J* = 8.4 Hz, 2H), 7.09 (s, 1H), 6.95 (dd, *J* = 1.7, 9.0 Hz, 1H), 5.10 (d, *J* = 3.3 Hz, 1H), 4.97 - 4.86 (m, 1H), 4.80 - 4.72 (m, 1H), 4.52 (d, *J* = 9.2 Hz, 1H), 4.43 (t, *J* = 7.9 Hz, 1H), 4.32 - 4.25 (m, 1H), 3.96 (t, *J* = 9.5 Hz, 2H), 3.74 (dd, *J* = 4.4, 10.3 Hz, 2H), 3.66 - 3.56 (m, 4H), 3.53 (s, 3H), 3.16 (s, 6H), 3.06 - 2.99 (m, 2H), 2.68 - 2.59 (m, 2H), 2.45 (s, 3H), 2.28 - 2.18 (m, 2H), 2.16 - 2.09 (m, 1H), 2.08 (s, 3H), 2.04 - 1.97 (m, 1H), 1.84 - 1.68 (m, 5H), 1.55 - 1.39 (m, 4H), 1.37 (d, *J* = 7.0 Hz, 3H), 1.29 - 1.19 (m, 2H), 0.94 (s, 9H).

1-(1-(1,3-Dimethoxypropan-2-yl)-2-(1,5-dimethyl-6-oxo-1,6-dihydropyridin-3-yl)-1*H*-benzo[*d*]imidazol-5-yl)-*N*-(16-(2-(((2*S*,4*R*)-1-((*S*)-2-(1-fluorocyclopropane-1-car-boxamido)-3,3-dimethylbutanoyl)-4-hydroxypyrrolidine-2-carboxamido)methyl)-5-(4-methylthiazol-5-yl)phe-noxy)hexadecyl)piperidine-4-carboxamide (8.9)

LCMS (Formic): R_t = 1.27 min, $[M+2H]^{2+}$ 612.3, 100% purity. ^{1}H NMR: (600 MHz, DMSO-d_6) δ 8.97 (s, 1H), 8.47 (t, *J* = 5.9 Hz, 1H), 7.99 (d, *J* = 1.5 Hz, 1H), 7.74 (t, *J* = 5.5 Hz, 1H), 7.66 - 7.63 (m, 1H), 7.60 (d, *J* = 8.8 Hz, 1H), 7.39 (d, *J* = 7.7 Hz, 1H), 7.30 - 7.26 (m, 1H), 7.08 (d, *J* = 1.8 Hz, 1H), 6.99 (s, 1H), 6.97 - 6.91 (m, 2H), 5.17 (d, *J* = 3.7 Hz, 1H), 4.79 - 4.73 (m, 1H), 4.59 (d, *J* = 9.2

Hz, 1H), 4.51 (t, *J* = 8.1 Hz, 1H), 4.38 - 4.33 (m, 1H), 4.28 (dd, *J* = 5.6, 16.2 Hz, 1H), 4.20 (dd, *J* = 5.6, 16.2 Hz, 1H), 4.03 (t, *J* = 6.2 Hz, 2H), 3.96 (t, *J* = 10.5 Hz, 2H), 3.74 (dd, *J* = 4.6, 10.5 Hz, 2H), 3.67 - 3.58 (m, 4H), 3.53 (s, 3H), 3.16 (s, 6H), 3.03 (dd, *J* = 6.8, 13.0 Hz, 2H), 2.67 - 2.59 (m, 2H), 2.45 (s, 3H), 2.26 - 2.18 (m, 1H), 2.11 - 2.05 (m, 4H), 1.97 - 1.88 (m, 1H), 1.80 - 1.67 (m, 6H), 1.49 - 1.19 (m, 30H), 0.95 (s, 9H). One exchangeable proton not observed.

1-(1-(1,3-Dimethoxypropan-2-yl)-2-(1,5-dimethyl-6-oxo-1,6-dihydropyridin-3-yl)-1*H*-benzo[*d*]imidazol-5-yl)-*N*-(12-(2-(((2*S*,4*R*)-4-hydroxy-1-((*S*)-3-methyl-2-(1-ox-oisoindolin-2-yl)butanoyl)pyrrolidine-2-carboxam-ido)methyl)-5-(4-methylthiazol-5-yl)phenoxy)dodecyl)-*N*-methylpiperidine-4-carboxamide (8.14)

LCMS (Formic): R_t = 1.10 min, $[M+2H]^{2+}$ 599.3, 97% purity. ^{1}H NMR: (600 MHz, DMSO-d_6) δ 8.97 (s, 1H), 8.38 - 8.32 (m, 1H), 7.99 (s, 1H), 7.71 (d, *J* = 7.3 Hz, 1H), 7.66 - 7.57 (m, 4H), 7.52 - 7.47 (m, 1H), 7.33 (d, *J* = 7.3 Hz, 1H), 7.08 (s, 1H), 7.02 - 6.92 (m, 3H), 5.09 (d, *J* = 3.3 Hz, 1H), 4.78 - 4.73 (m, 1H), 4.71 (d, *J* = 10.3 Hz, 1H), 4.54 (d, *J* = 17.9 Hz, 1H), 4.45 (d, *J* = 17.9 Hz, 1H), 4.42 - 4.38 (m, 1H), 4.36 - 4.18 (m, 3H), 4.08 - 4.01 (m, 2H), 3.98 - 3.93 (m, 2H), 3.80 - 3.65 (m, 4H), 3.62 (d, *J* = 11.7 Hz, 2H), 3.52 (d, *J* = 4.0 Hz, 3H), 3.29 - 3.23 (m, 2H), 3.18 - 3.13 (m, 6H), 3.01 (s, 1.5H), 2.79 (s, 1.5 H), 2.74 - 2.64 (m, 3H), 2.47 - 2.45 (m, 3H), 2.36 - 2.29 (m, 1H), 2.09 - 2.00 (m, 4H), 1.95 - 1.89 (m, 1H), 1.81 - 1.65 (m, 6H), 1.55 - 1.13 (m, 18H), 0.98 - 0.93 (m, 3H), 0.75 - 0.71 (m, 3H).

1-(1-(1,3-Dimethoxypropan-2-yl)-2-(1,5-dimethyl-6-oxo-1,6-dihydropyridin-3-yl)-1*H*-benzo[*d*]imidazol-5-yl)-*N*-(12-(((*S*)-1-((2*S*,4*R*)-4-hydroxy-2-((4-(4-methylthiazol-5-yl)benzyl)carbamoyl)pyrrolidin-1-yl)-3,3-dimethyl-1-oxobutan-2-yl)amino)-12-oxododecyl)-*N*-methylpiperi-dine-4-carboxamide (8.38)

LCMS (Formic): R_t = 0.95 min, $[(M+H)]^{2+}$ 547.2, 100% purity. ^{1}H NMR: (600 MHz, DMSO-d_6) δ 8.98 (s, 1H), 8.59 - 8.52 (m, 1H), 8.01 (s, 1H), 7.83 (d, *J* = 9.2 Hz, 1H), 7.66 (s, 1H), 7.61 (d, *J* = 9.2 Hz, 1H), 7.46 - 7.35 (m, 4H), 7.09 (d, *J* = 2.0, 1H), 6.96 (dd, *J* = 2.0, 9.0 Hz, 1H), 5.12 (d, *J* = 3.7 Hz, 1H), 4.81 - 4.72 (m, 1H), 4.55 (d, *J* = 9.2 Hz, 1H), 4.46 - 4.41 (m, 2H), 4.35 (s, 1H), 4.22 (dd, *J* = 5.3, 15.6 Hz, 1H), 3.97 (t, *J* = 9.5 Hz, 2H), 3.75 (dd, *J* = 4.8, 10.3 Hz, 2H), 3.70 - 3.60 (m, 4H), 3.54 (s, 3H), 3.27 (t, *J* = 7.2 Hz, 1H), 3.17 (s, 6H), 3.03 (s, 1.5H), 2.80 (s, 1.5H), 2.75 - 2.67 (m, 3H), 2.45 (s, 3H), 2.29 - 2.23 (m, 1H), 2.13 - 2.10 (m, 1H), 2.09 (s, 3H), 2.05 - 2.01 (m, 1H), 1.94 - 1.89 (m, 1H), 1.82 - 1.65 (m, 4H), 1.56 - 1.40 (m, 4H), 1.32 - 1.18 (m, 15H), 0.94 (s, 9H).

1-(1-(1,3-Dimethoxypropan-2-yl)-2-(1,5-dimethyl-6-oxo-1,6-dihydropyridin-3-yl)-1*H*-benzo[*d*]imidazol-5-yl)-*N*-(8-((2-(2,6-dioxopiperidin-3-yl)-1,3-dioxoisoindolin-4-yl)oxy)octyl)piperidine-4-carboxamide (8.55)

LCMS (Formic): R_t = 0.81 min, $[M+H]^+$ 852.6, 93% purity. ^{1}H NMR: (600 MHz, DMSO-d_6) δ 11.07 (s, 1H), 7.99 (s, 1H), 7.80 (t, *J* = 7.9 Hz, 1H), 7.75 (t, *J* = 5.3 Hz, 1H), 7.64 (s, 1H), 7.60 (d, *J* = 8.8 Hz, 1H), 7.51 (d, *J* = 8.8 Hz, 1H), 7.43 (d, *J* = 7.3 Hz, 1H), 7.08 (s, 1H), 6.95 - 6.92 (m, 1H), 5.08 (dd, *J* = 5.5, 12.8 Hz, 1H), 4.80 - 4.70 (m, 1H), 4.20 (t, *J* = 6.4 Hz, 2H), 3.96 (t, *J* = 9.5 Hz, 2H), 3.74 (dd, *J* = 4.4, 10.3 Hz, 2H), 3.61 (d, *J* = 12.1 Hz, 2H), 3.53 (s, 3H), 3.16 (s, 6H), 3.07 - 3.01 (m, 2H), 2.93 - 2.82 (m, 1H), 2.66 - 2.52 (m, 4H), 2.26 - 2.17 (m, 1H), 2.08 (s, 3H), 2.06 - 1.98 (m, 1H), 1.79 - 1.68 (m, 6H), 1.50 - 1.22 (m, 10H).

1-(1-(1,3-Dimethoxypropan-2-yl)-2-(1,5-dimethyl-6-oxo-1,6-dihydropyridin-3-yl)-1*H*-benzo[*d*]imidazol-5-yl)-

14

N-(9-(((S)-1-((2S,4R)-4-hydroxy-2-(((S)-1-(4-(4-methyl-thiazol-5-yl)phenyl)ethyl)carbamoyl)pyrrolidin-1-yl)-3,3-dimethyl-1-oxobutan-2-yl)amino-9-oxononyl)piperi-dine-4-carboxamide (8.61)

LCMS (Formic): R$_t$ = 0.84 min, [M+2H]$^{2+}$ 526.2, 100% purity. ^{1}H NMR: (600 MHz, DMSO-d_6) δ 8.98 (s, 1H), 8.37 (d, J = 7.7 Hz, 1H), 8.00 (s, 1H), 7.79 - 7.74 (m, 2H), 7.65 (s, 1H), 7.61 (d, J = 8.4 Hz, 1H), 7.45 - 7.42 (m, J = 8.4 Hz, 2H), 7.41 - 7.36 (m, J = 8.1 Hz, 2H), 7.10 (s, 1H), 6.95 (d, J = 7.3 Hz, 1H), 5.10 (d, J = 3.3 Hz, 1H), 4.97 - 4.87 (m, 1H), 4.80 - 4.73 (m, 1H), 4.53 (d, J = 9.2 Hz, 1H), 4.43 (t, J = 7.9 Hz, 1H), 4.33 - 4.25 (m, 1H), 3.97 (t, J = 9.5 Hz, 2H), 3.75 (dd, J = 4.4, 10.3 Hz, 2H), 3.67 - 3.57 (m, 4H), 3.54 (s, 3H), 3.17 (s, 6H), 3.08 - 3.00 (m, 2H), 2.70 - 2.60 (m, 2H), 2.46 (s, 3H), 2.30 - 2.20 (m, 2H), 2.17 - 2.11 (m, 1H), 2.09 (s, 3H), 2.06 - 1.97 (m, 1H), 1.84 - 1.69 (m, 5H), 1.56 - 1.35 (m, 6H), 1.30 - 1.19 (m, 9H), 0.95 (s, 9H).

1-(1,3-Dimethoxypropan-2-yl)-2-(1,5-dimethyl-6-oxo-1,6-dihydropyridin-3-yl)-N-(17-(2-(((2S,4R)-1-((S)-2-(1-fluorocyclopropane-1-carboxamido)-3,3-dimethylbuta-noyl)-4-hydroxypyrrolidine-2-carboxamido)methyl)-5-(4-methylthiazol-5-yl)phenoxy)-3,6,9,12,15-pentaoxa-heptadecyl)-1H-benzo[d]imidazole-5-carboxamide (9.1)

LCMS (Formic): R$_t$ = 0.92 min, [M+2H]$^{2+}$ 582.6, 100% purity. ^{1}H NMR (600 MHz, DMSO-d_6) δ 8.98 (s, 1H), 8.56 – 8.44 (m, 2H), 8.17 (br s, 1H), 8.07 (br s, 1H), 7.86 (d, J = 8.8 Hz, 1H), 7.76 (br d, J = 8.8 Hz, 1H), 7.69 (br s, 1H), 7.41 (br d, J = 7.7 Hz, 1H), 7.29 (br d, J = 8.8 Hz, 1H), 7.04 (br s, 1H), 6.97 (br d, J = 7.7 Hz, 1H), 5.18 (br d, J = 3.3 Hz, 1H), 4.92 – 4.80 (m, 1H), 4.60 (br d, J = 9.5 Hz, 1H), 4.52 (t, J = 7.7 Hz, 1H), 4.36 (br s, 1H), 4.34 – 4.27 (m, 1H), 4.26 – 4.14 (m, 3H), 4.14 – 4.07 (m, 1H), 4.06 – 4.00 (m, 2H), 3.82 – 3.73 (m, 4H), 3.71 – 3.58 (m, 4H), 3.58 – 3.41 (m, 20H), 3.19 – 3.17 (m, 1H), 3.16 (s, 6H), 2.46 (s, 3H), 2.10 (s, 3H), 1.99 – 1.88 (m, 1H), 1.45 – 1.30 (m, 2H), 1.28 – 1.18 (m, 2H), 0.96 (s, 9H).

1-(1,3-Dimethoxypropan-2-yl)-2-(1,5-dimethyl-6-oxo-1,6-dihydropyridin-3-yl)-N-(6-(((S)-1-((2S,4R)-4-hydroxy-2-(((S)-1-(4-(4-methylthiazol-5-yl)phenyl)ethyl)car-bamoyl)pyrrolidin-1-yl)-3,3-dimethyl-1-oxobutan-2-yl)amino)-6-oxohexyl)-1H-benzo[d]imidazole-5-carbox-amide (9. 8)

LCMS (Formic): R$_t$ = 0.89 min, [M+2H]$^{2+}$ 463.6, 100% purity. ^{1}H NMR (600 MHz, DMSO-d_6) δ 8.97 (s, 1H), 8.43 (t, J = 5.5 Hz, 1H), 8.36 (d, J = 7.7 Hz, 1H), 8.14 (s, 1H), 8.06 (d, J = 1.5 Hz, 1H), 7.84 (d, J = 8.4 Hz, 1H), 7.78 (br d, J = 9.2 Hz, 1H), 7.74 (dd, J = 8.8, 1.1 Hz, 1H), 7.68 (s, 1H), 7.43 (d, J = 8.4 Hz, 2H), 7.37 (d, J = 8.4 Hz, 2H), 5.11 (d, J = 3.3 Hz, 1H), 4.91 (br t, J = 7.3 Hz, 1H), 4.88 – 4.83 (m, 1H), 4.51 (d, J = 9.5 Hz, 1H), 4.42 (t, J = 8.1 Hz, 1H), 4.30 – 4.25 (m, 1H), 4.03 (t, J = 9.7 Hz, 2H), 3.77 (dd, J = 10.3, 4.0 Hz, 2H), 3.64 – 3.56 (m, 2H), 3.54 (s, 3H), 3.30 – 3.23 (m, 2H), 3.18 – 3.13 (m, 6H), 2.54 (s, 1H), 2.45 (s, 3H), 2.30 – 2.22 (m, 1H), 2.18 – 2.10 (m, 1H), 2.09 (s, 3H), 2.03 – 1.96 (m, 1H), 1.79 (ddd, J = 12.7, 8.3, 5.0 Hz, 1H), 1.58 – 1.45 (m, 4H), 1.37 (d, J = 7.0 Hz, 2H), 1.34 – 1.27 (m, 2H), 0.94 – 0.89 (m, 9H).

1-(1,3-Dimethoxypropan-2-yl)-2-(1,5-dimethyl-6-oxo-1,6-dihydropyridin-3-yl)-N-(16-(2-(((2S,4R)-1-((S)-2-(1-fluorocyclopropane-1-carboxamido)-3,3-dimethylbuta-noyl)-4-hydroxypyrrolidine-2-carboxamido)methyl)-5-(4-methylthiazol-5-yl)phenoxy)hexadecyl)-1H-benzo[d]imidazole-5-carboxamide (9.9)

LCMS (Formic): R$_t$ = 1.53 min, [M+2H]$^{2+}$ 570.7, 100% purity. ^{1}H NMR (600 MHz, DMSO-d_6) δ 8.97 (s, 1H), 8.47 (t, J = 6.2 Hz,

1H), 8.42 (br t, J = 5.3 Hz, 1H), 8.14 (s, 1H), 8.06 (s, 1H), 7.84 (d, J = 8.4 Hz, 1H), 7.73 (br d, J = 8.8 Hz, 1H), 7.68 (s, 1H), 7.39 (d, J = 7.7 Hz, 1H), 7.28 (br d, J = 8.8 Hz, 1H), 6.99 (s, 1H), 6.94 (d, J = 7.3 Hz, 1H), 5.17 (br d, J = 2.2 Hz, 1H), 4.90 – 4.82 (m, 1H), 4.59 (d, J = 9.2 Hz, 1H), 4.51 (t, J = 7.9 Hz, 1H), 4.35 (br s, 1H), 4.28 (br dd, J = 16.3, 5.7 Hz, 1H), 4.19 (dd, J = 16.1, 5.1 Hz, 1H), 4.07 – 3.99 (m, 4H), 3.77 (dd, J = 10.1, 4.2 Hz, 2H), 3.65 (dd, J = 11.4, 4.4 Hz, 1H), 3.60 (br d, J = 10.6 Hz, 1H), 3.54 (s, 3H), 3.27 (q, J = 6.2 Hz, 2H), 3.18 – 3.14 (m, 6H), 2.45 (s, 3H), 2.12 – 2.05 (m, 4H), 1.96 – 1.89 (m, 1H), 1.78 – 1.70 (m, 2H), 1.57 – 1.49 (m, 2H), 1.47 – 1.40 (m, 2H), 1.40 – 1.21 (m, 26H), 0.95 (s, 9H)

1-(1,3-Dimethoxypropan-2-yl)-2-(1,5-dimethyl-6-oxo-1,6-dihydropyridin-3-yl)-N-(2-(2-(2-(2-((2-(2,6-dioxopi-peridin-3-yl)-1-oxoisoindolin-4-yl)amino)-2-oxoeth-oxy)ethoxy)ethoxy)ethyl)-1H-benzo[d]imidazole-5-car-boxamide (9.51)

LCMS (Formic): R$_t$ = 0.69 min, [M+H]$^+$ 816.5, 92% purity. ^{1}H NMR (600 MHz, DMSO-d_6) δ 10.99 (br s, 1H), 9.69 (s, 1H), 8.51 – 8.47 (m, 1H), 8.15 (s, 1H), 8.06 (s, 1H), 7.85 (br d, J = 8.4 Hz, 1H), 7.73 (br t, J = 7.9 Hz, 2H), 7.67 (s, 1H), 7.55 (d, J = 8.4 Hz, 1H), 7.52 – 7.48 (m, 1H), 5.13 (br dd, J = 13.6, 4.8 Hz, 1H), 4.88 – 4.82 (m, 1H), 4.37 (q, J = 18.0 Hz, 2H), 4.16 – 4.11 (m, 2H), 4.02 (br t, J = 9.9 Hz, 2H), 3.76 (br dd, J = 10.3, 4.0 Hz, 2H), 3.67 (br d, J = 3.7 Hz, 2H), 3.62 (d, J = 3.7 Hz, 2H), 3.59 – 3.52 (m, 9H), 3.43 (br d, J = 5.5 Hz, 2H), 3.17 (br d, J = 2.9 Hz, 1H), 3.15 (s, 6H), 2.94 – 2.86 (m, 1H), 2.59 (br d, J = 16.9 Hz, 1H), 2.09 (s, 3H), 2.03 – 1.97 (m, 1H)

1-(1,3-Dimethoxypropan-2-yl)-2-(1,5-dimethyl-6-oxo-1,6-dihydropyridin-3-yl)-N-(8-((2-(2,6-dioxopiperidin-3-yl)-1,3-dioxoisoindolin-4-yl)oxy)octyl)-1H-benzo[d]imid-azole-5-carboxamide (9.55)

LCMS (Formic): R$_t$ = 0.99 min, [M+H]$^+$ 769.5, 94% purity. ^{1}H NMR (600 MHz, DMSO-d_6) δ 11.08 (br s, 1H), 8.45 – 8.41 (m, 1H), 8.14 (s, 1H), 8.06 (d, J = 1.6 Hz, 1H), 7.84 (d, J = 8.8 Hz, 1H), 7.81 – 7.77 (m, 1H), 7.73 (dd, J = 8.4, 1.6 Hz, 1H), 7.67 (br s, 1H), 7.50 (d, J = 8.4 Hz, 1H), 7.43 (d, J = 7.0 Hz, 1H), 5.07 (dd, J = 12.8, 5.5 Hz, 1H), 4.90 – 4.81 (m, 1H), 4.19 (t, J = 6.2 Hz, 2H), 4.02 (t, J = 9.9 Hz, 2H), 3.77 (dd, J = 10.3, 4.4 Hz, 2H), 3.54 (s, 3H), 3.28 (q, J = 6.4 Hz, 2H), 3.18 – 3.16 (m, 1H), 3.15 (s, 6H), 2.91 – 2.82 (m, 1H), 2.61 – 2.55 (m, 1H), 2.09 (s, 3H), 2.05 – 1.99 (m, 1H), 1.78 – 1.73 (m, 2H), 1.59 – 1.51 (m, 2H), 1.49 – 1.43 (m, 2H), 1.34 (br s, 6H)

1-(1,3-Dimethoxypropan-2-yl)-2-(1,5-dimethyl-6-oxo-1,6-dihydropyridin-3-yl)-N-(10-((2-(2,6-dioxopiperidin-3-yl)-1,3-dioxoisoindolin-4-yl)oxy)decyl)-1H-benzo[d]im-idazole-5-carboxamide (9.56)

LCMS (Formic): R$_t$ = 1.09 min, [M+H]$^+$ 797.6, 96% purity. ^{1}H NMR (600 MHz, DMSO-d_6) δ 11.10 (br s, 1H), 8.44 – 8.40 (m, 1H), 8.14 (s, 1H), 8.06 (d, J = 2.2 Hz, 1H), 7.84 (d, J = 9.2 Hz, 1H), 7.79 (t, J = 7.9 Hz, 1H), 7.73 (dd, J = 9.2, 1.1 Hz, 1H), 7.68 (br s, 1H), 7.50 (d, J = 8.8 Hz, 1H), 7.43 (d, J = 7.3 Hz, 1H), 5.07 (dd, J = 12.8, 5.5 Hz, 1H), 4.89 – 4.83 (m, 1H), 4.19 (br t, J = 6.2 Hz, 2H), 4.02 (t, J = 9.9 Hz, 2H), 3.77 (dd, J = 10.6, 4.4 Hz, 2H), 3.54 (s, 3H), 3.27 (q, J = 7.0 Hz, 2H), 3.18 – 3.14 (m, 7H), 2.92 – 2.83 (m, 1H), 2.62 – 2.55 (m, 1H), 2.09 (s, 3H), 2.06 – 1.99 (m, 1H), 1.78 – 1.71 (m, 2H), 1.57 – 1.51 (m, 2H), 1.48 – 1.42 (m, 2H), 1.34 – 1.28 (m, 10H)

(2S,4R)-N-(2-((1-(2-(1,5-Dimethyl-6-oxo-1,6-dihydro-pyridin-3-yl)-5-morpholino-1H-benzo[d]imidazol-1-yl)-2-oxo-6,9,12,15,18-pentaoxa-3-azaicosan-20-yl)oxy)-4-(4-methylthiazol-5-yl)benzyl)-1-((S)-2-(1-

15

fluorocyclopropane-1-carboxamido)-3,3-dimethylbuta-noyl)-4-hydroxypyrrolidine-2-carboxamide (10.1)

LCMS (Formic): R_t = 0.96 min, [M+2H]$^{2+}$ 581.3, 100% purity. ^{1}H NMR (400 MHz, DMSO-d_6) δ 8.97 (s, 1H), 8.53 (t, J = 5.4 Hz, 1H), 8.46 (t, J = 5.9 Hz, 1H), 8.06 (d, J = 2.5 Hz, 1H), 7.68 (dd, J = 2.5, 1.5 Hz, 1H), 7.40 (d, J = 7.9 Hz, 1H), 7.33 (d, J = 8.9 Hz, 1H), 7.27 (dd, J = 9.4, 3.0 Hz, 1H), 7.11 (d, J = 2.0 Hz, 1H), 7.03 (d, J = 1.5 Hz, 1H), 7.00 (dd, J = 8.9, 2.5 Hz, 1H), 6.96 (dd, J = 7.9, 1.5 Hz, 1H), 5.15 (d, J = 3.4 Hz, 1H), 4.86 (s, 2H), 4.59 (d, J = 8.9 Hz, 1H), 4.52 (t, J = 8.4 Hz, 1H), 4.38 – 4.33 (m, 1H), 4.29 (d, J = 5.9 Hz, 1H), 4.22 (d, J = 5.4 Hz, 1H), 4.20 – 4.15 (m, 2H), 4.07 (q, J = 4.9 Hz, 1H), 3.81 – 3.73 (m, 6H), 3.68 – 3.57 (m, 4H), 3.56 – 3.48 (m, 16H), 3.43 (t, J = 5.9 Hz, 2H), 3.29 – 3.24 (m, 2H), 3.11 – 3.04 (m, 4H), 2.47 – 2.43 (m, 3H), 2.12 – 2.06 (m, 4H), 1.92 (ddd, J = 12.9, 8.5, 4.7 Hz, 1H), 1.42 – 1.30 (m, 2H), 1.22 (dd, J = 8.4, 3.4 Hz, 2H), 0.96 (s, 9H).

(2S,4R)-N-(2-((12-(2-(2-(1,5-Dimethyl-6-oxo-1,6-dihy-dropyridin-3-yl)-5-morpholino-1H-benzo[d]imidazol-1-yl)-N-methylacetamido)dodecyl)oxy)-4-(4-methylthiazol-5-yl)benzyl)-4-hydroxy-1-((S)-3-methyl-2-(1-oxoisoin-dolin-2-yl)butanoyl)pyrrolidine-2-carboxamide (10.14)

LCMS (Formic): R_t = 1.31 min, [M+2H]$^{2+}$ 556.3, 92% purity. ^{1}H NMR (400 MHz, DMSO-d_6) δ 8.98 (s, 1H), 8.34 (t, J = 5.4 Hz, 1H), 7.94 – 7.88 (m, 1H), 7.71 (d, J = 7.4 Hz, 1H), 7.61 (d, J = 3.4 Hz, 2H), 7.59 – 7.55 (m, 1H), 7.51 – 7.47 (m, 1H), 7.36 – 7.27 (m, 2H), 7.10 (d, J = 2.0 Hz, 1H), 7.02 – 6.94 (m, 3H), 5.23 – 5.14 (m, 2H), 5.07 (br d, J = 2.0 Hz, 1H), 4.71 (d, J = 10.8 Hz, 1H), 4.58 – 4.43 (m, 2H), 4.40 (d, J = 7.4 Hz, 1H), 4.36 – 4.18 (m, 3H), 4.04 (t, J = 6.2 Hz, 2H), 3.80 – 3.74 (m, 5H), 3.68 (d, J = 10.3 Hz, 1H), 3.50 (d, J = 1.5 Hz, 3H), 3.39 – 3.33 (m, 1H), 3.28 – 3.25 (m, 1H), 3.08 – 3.05 (m, 5H), 2.82 (s, 1H), 2.47 (s, 3H), 2.38 – 2.27 (m, 1H), 2.09 – 2.00 (m, 4H), 1.97 – 1.88 (m, 1H), 1.81 – 1.68 (m, 2H), 1.54 (br s, 1H), 1.49 – 1.13 (m, 18H), 0.96 (d, J = 6.7 Hz, 3H), 0.73 (d, J = 6.7 Hz, 3H). Note: rotamers observed.

(2S,4R)-1-((S)-2-(16-(2-(2-(1,5-Dimethyl-6-oxo-1,6-di-hydropyridin-3-yl)-5-morpholino-1H-benzo[d]imidazol-1-yl)acetamido)hexadecanamido)-3,3-dimethylbuta-noyl)-4-hydroxy-N-((S)-1-(4-(4-methylthiazol-5-yl)phe-nyl)ethyl)pyrrolidine-2-carboxamide (10.30)

LCMS (Formic): R_t = 1.31 min, [M+2H]$^{2+}$ 532.4, 95% purity. ^{1}H NMR (400 MHz, DMSO-d_6) δ 8.98 (s, 1H), 8.41 (t, J = 5.7 Hz, 1H), 8.34 (d, J = 7.9 Hz, 1H), 8.10 (d, J = 2.0 Hz, 1H), 7.74 (d, J = 9.4 Hz, 1H), 7.68 (dd, J = 2.5, 1.0 Hz, 1H), 7.45 – 7.41 (m, 2H), 7.40 – 7.31 (m, 3H), 7.11 (d, J = 2.5 Hz, 1H), 6.99 (dd, J = 8.9, 2.0 Hz, 1H), 5.08 (br s, 1H), 4.96 – 4.87 (m, 1H), 4.84 (s, 2H), 4.51 (d, J = 9.4 Hz, 1H), 4.42 (t, J = 7.9 Hz, 1H), 4.28 (br s, 1H), 3.81 – 3.73 (m, 4H), 3.61 (br d, J = 4.4 Hz, 2H), 3.51 (s, 3H), 3.12 – 3.04 (m, 6H), 2.45 (s, 3H), 2.29 – 2.18 (m, 1H), 2.13 – 2.03 (m, 4H), 1.99 (br dd, J = 7.6, 2.7 Hz, 1H), 1.80 (ddd, J = 12.9, 8.2, 4.9 Hz, 1H), 1.52 – 1.42 (m, 2H), 1.41 – 1.34 (m, 5H), 1.23 (s, 22H), 0.93 (s, 9H)

2-(2-(1,5-Dimethyl-6-oxo-1,6-dihydropyridin-3-yl)-5-morpholino-1H-benzo[d]imidazol-1-yl)-N-(12-((2-(2,6-di-oxopiperidin-3-yl)-1,3-dioxoisoindolin-4-yl)oxy)do-decyl)acetamide (10.35)

LCMS (Formic): R_t = 0.99 min, [M+H]$^+$ 822.7, 88% purity. ^{1}H NMR (400 MHz, DMSO-d_6) δ 8.42 (t, J = 5.7 Hz, 1H), 8.10 (d, J = 2.5 Hz, 1H), 7.82 – 7.76 (m, 1H), 7.68 (dd, J = 2.5, 1.5 Hz, 1H), 7.53 – 7.47 (m, 1H), 7.46 – 7.41 (m, 1H), 7.33 (d, J = 8.9 Hz, 1H), 7.11 (d, J = 2.0 Hz, 1H), 6.99 (dd, J = 8.9, 2.0 Hz, 1H), 5.07 (dd, J = 12.8, 5.4 Hz, 1H), 4.84 (s, 2H), 4.19 (t, J = 6.4 Hz, 2H), 3.83 –

3.70 (m, 4H), 3.51 (s, 3H), 3.17 (br s, 2H), 3.13 – 3.05 (m, 5H), 2.96 – 2.79 (m, 1H), 2.61 – 2.55 (m, 1H), 2.07 (s, 3H), 2.05 – 1.98 (m, 1H), 1.79 – 1.70 (m, 2H), 1.47 – 1.23 (m, 18H). Note: one N-H not observed.

2-(2-(1,5-Dimethyl-6-oxo-1,6-dihydropyridin-3-yl)-5-morpholino-1H-benzo[d]imidazol-1-yl)-N-(8-((2-(2,6-di-oxopiperidin-3-yl)-1,3-dioxoisoindolin-4-yl)oxy)octyl)ac-etamide (10.55)

LCMS (Formic): R_t = 0.80 min, [M+H]$^+$ 766.7, 81% purity. ^{1}H NMR (400 MHz, DMSO-d_6) δ 11.02 (br s, 1H), 8.41 (t, J = 5.4 Hz, 1H), 8.10 (d, J = 2.5 Hz, 1H), 7.83 – 7.73 (m, 1H), 7.69 – 7.67 (m, 1H), 7.50 (d, J = 8.4 Hz, 1H), 7.46 – 7.41 (m, 1H), 7.33 (d, J = 8.9 Hz, 1H), 7.11 (d, J = 2.0 Hz, 1H), 7.00 (dd, J = 8.9, 2.5 Hz, 1H), 5.07 (dd, J = 13.0, 5.7 Hz, 1H), 4.85 (s, 2H), 4.19 (t, J = 6.4 Hz, 2H), 3.76 (dd, J = 5.8, 4.3 Hz, 4H), 3.51 (s, 3H), 3.17 (s, 1H), 3.13 – 3.04 (m, 6H), 2.96 – 2.78 (m, 1H), 2.61 – 2.54 (m, 1H), 2.07 (s, 3H), 2.06 – 1.98 (m, 1H), 1.82 – 1.63 (m, 2H), 1.50 – 1.36 (m, 4H), 1.33 – 1.21 (m, 6H)

2-(2-(1,5-Dimethyl-6-oxo-1,6-dihydropyridin-3-yl)-5-morpholino-1H-benzo[d]imidazol-1-yl)-N-(10-((2-(2,6-di-oxopiperidin-3-yl)-1,3-dioxoisoindolin-4-yl)oxy)decyl)ac-etamide (10.56)

LCMS (Formic): R_t = 0.89 min, [M+H]$^+$ 794.7, 87% purity. ^{1}H NMR (400 MHz, DMSO-d_6) δ 8.41 (t, J = 5.7 Hz, 1H), 8.10 (d, J = 2.0 Hz, 1H), 7.80 (dd, J = 8.6, 7.1 Hz, 1H), 7.68 (dd, J = 2.5, 1.0 Hz, 1H), 7.50 (d, J = 8.4 Hz, 1H), 7.43 (d, J = 6.9 Hz, 1H), 7.33 (d, J = 8.9 Hz, 1H), 7.11 (d, J = 2.0 Hz, 1H), 7.00 (dd, J = 8.9, 2.5 Hz, 1H), 5.07 (dd, J = 12.8, 5.4 Hz, 1H), 4.84 (s, 2H), 4.19 (t, J = 6.4 Hz, 2H), 3.79 – 3.74 (m, 4H), 3.51 (s, 3H), 3.17 (br s, 1H), 3.13 – 3.04 (m, 7H), 2.92 – 2.81 (m, 1H), 2.61 – 2.52 (m, 2H), 2.07 (s, 3H), 2.06 – 1.98 (m, 1H), 1.79 – 1.70 (m, 2H), 1.48 – 1.26 (m, 12H). Note: one N-H not observed.

ASSOCIATED CONTENT

Supporting Information – containing additional chemistry optimisation experiments and associated data, data for the HER2 and BRD4 libraries including LCMS purities/conversions and assay results.

AUTHOR INFORMATION

Corresponding Author

*Email: john.d.harling@gsk.com

Author Contributions

#R.S. and E.B-M. contributed equally.

ACKNOWLEDGEMENT

ABBREVIATIONS

16

BRD4, bromodomain-containing protein 4; bRo5, beyond rule of 5; chromlogD, chromatographic logD; CTG, Cell-Titer Glo; COMU, (1-cyano-2-ethoxy-2-oxoethylidenaminooxy)dimethyl-amino-morpholino-carbenium hexafluorophosphate; D2B, direct-to-biology; DCM, dichloromethane; DIC, *N,N'*-diisopropyl-carbodiimide; DIPEA, *N,N*-diisopropylethylamine; DMF, *N,N'*-dimethylformamide; DMSO, dimethyl sulfoxide; EDC.HCl, 1-ethyl-3-(3-dimethylaminopropyl)carbodiimide hydrochloride; FRET, fluorescence resonance energy transfer; HATU, hex-afluorophosphate azabenzotriazole tetramethyl uronium ; HER2, human epidermal growth factor receptor 2; HTE, high-throughput experimentation; NHS, *N*-hydroxysuccinimide; NMM, *N*-methyl morpholine; LCMS, liquid-chromatography mass-spectrometry; MDAP, mass-directed automated purification; MoA, mode/mechanism of action; PDCP, phenyl dichloro-phosphate; PEG, polyethylene glycol; POI, protein-of-interest; PROTAC, proteolysis targeting chimera; SAR, structure-activity relationships; SCX, strong cation exchange; TCFH, chloro-*N,N,N',N'*-tetramethylformamidinium hexafluorophosphate; TFA, trifluoroacetic acid; TSTU, *O*-(*N*-succinimidyl)-*N,N,N',N'*-tetramethyluronium tetrafluoroborate; VHL, Von Hippel-Lindau.

REFERENCES

1. Sakamoto, K. M.; Kim, K. B.; Kumagai, A.; Mercurio, F.; Crews, C. M.; Deshaies, R. J., Protacs: chimeric molecules that target proteins to the Skp1-Cullin-F box complex for ubiquitination and degradation. *Proc. Natl. Acad. Sci. USA* 2001, *98* (15), 8554-8559.
2. Chirnomas, D.; Hornberger, K. R.; Crews, C. M., Protein degraders enter the clinic - a new approach to cancer therapy. *Nat Rev Clin Oncol* 2023, *20* (4), 265-278.
3. Mullard, A., Targeted protein degraders crowd into the clinic. *Nat. Rev. Drug Discov.* 2021, *20* (4), 247-250.
4. Garber, K., The PROTAC gold rush. *Nature Biotechnology* 2022, *40* (1), 12-16.
5. Winter Georg, E.; Buckley Dennis, L.; Paulk, J.; Roberts Justin, M.; Souza, A.; Dhe-Paganon, S.; Bradner James, E., Phthalimide conjugation as a strategy for in vivo target protein degradation. *Science* 2015, *348* (6241), 1376-1381.
6. Bondeson, D. P.; Mares, A.; Smith, I. E. D.; Ko, E.; Campos, S.; Miah, A. H.; Mulholland, K. E.; Routly, N.; Buckley, D. L.; Gustafson, J. L.; Zinn, N.; Grandi, P.; Shimamura, S.; Bergamini, G.; Faelth-Savitski, M.; Bantscheff, M.; Cox, C.; Gordon, D. A.; Willard, R. R.; Flanagan, J. J.; Casillas, L. N.; Votta, B. J.; den Besten, W.; Famm, K.; Kruidenier, L.; Carter, P. S.; Harling, J. D.; Churcher, I.; Crews, C. M., Catalytic in vivo protein knockdown by small-molecule PROTACs. *Nat. Chem. Biol.* 2015, *11* (8), 611-617.
7. Bondeson, D. P.; Smith, B. E.; Burslem, G. M.; Buhimschi, A. D.; Hines, J.; Jaime-Figueroa, S.; Wang, J.; Hamman, B. D.; Ishchenko, A.; Crews, C. M., Lessons in PROTAC Design from Selective Degradation with a Promiscuous Warhead. *Cell Chem. Biol.* 2018, *25* (1), 78-87.
8. Cantrill, C.; Chaturvedi, P.; Rynn, C.; Petrig Schaffland, J.; Walter, I.; Wittwer, M. B., Fundamental aspects of DMPK optimization of targeted protein degraders. *Drug Discov. Today* 2020, *25* (6), 969-982.
9. Kofink, C.; Trainor, N.; Mair, B.; Wohrle, S.; Wurm, M.; Mischerikow, N.; Roy, M. J.; Bader, G.; Greb, P.; Garavel, G.; Diers, E.; McLennan, R.; Whitworth, C.; Vetma, V.; Rumpel, K.; Scharnweber, M.; Fuchs, J. E.; Gerstberger, T.; Cui, Y.; Gremel, G.; Chetta, P.; Hopf, S.; Budano, N.; Rinnenthal, J.; Gmaschitz, G.; Mayer, M.; Koegl, M.; Ciulli, A.; Weinstabl, H.; Farnaby, W., A selective and orally bioavailable VHL-recruiting PROTAC achieves SMARCA2 degradation in vivo. *Nat Commun* 2022, *13* (1), 5969.
10. Poongavanam, V.; Atilaw, Y.; Siegel, S.; Giese, A.; Lehmann, L.; Meibom, D.; Erdelyi, M.; Kihlberg, J., Linker-Dependent Folding Rationalizes PROTAC Cell Permeability. *Journal of Medicinal Chemistry* 2022, *65* (19), 13029-13040.

11. Imrie, F.; Bradley, A. R.; van der Schaar, M.; Deane, C. M., Deep Generative Models for 3D Linker Design. *J. Chem. Inf. Model.* 2020, *60* (4), 1983-1995.
12. Zhu, C. L.; Luo, X.; Tian, T.; Rao, Z.; Wang, H.; Zhou, Z.; Mi, T.; Chen, D.; Xu, Y.; Wu, Y.; Che, J.; Zhou, Y.; Li, J.; Dong, X., Structure-based rational design enables efficient discovery of a new selective and potent AKT PROTAC degrader. *Eur J Med Chem* 2022, *238*, 114459.
13. Liu, X.; Ciulli, A., Proximity-Based Modalities for Biology and Medicine. *ACS Cent Sci* 2023, *9* (7), 1269-1284.
14. Thomas, R. P.; Heap, R. E.; Zappacosta, F.; Grant, E. K.; Pogany, P.; Besley, S.; Fallon, D. J.; Hann, M. M.; House, D.; Tomkinson, N. C. O.; Bush, J. T., A direct-to-biology high-throughput chemistry approach to reactive fragment screening. *Chem Sci* 2021, *12* (36), 12098-12106.
15. Buitrago Santanilla, A.; Regalado, E. L.; Pereira, T.; Shevlin, M.; Bateman, K.; Campeau, L. C.; Schneeweis, J.; Berritt, S.; Shi, Z. C.; Nantermet, P.; Liu, Y.; Helmy, R.; Welch, C. J.; Vachal, P.; Davies, I. W.; Cernak, T.; Dreher, S. D., Nanomole-scale high-throughput chemistry for the synthesis of complex molecules. *Science* 2015, *347* (6217), 49-53.
16. Hendrick, C. E.; Jorgensen, J. R.; Chaudhry, C.; Strambeanu, II; Brazeau, J. F.; Schiffer, J.; Shi, Z.; Venable, J. D.; Wolkenberg, S. E., Direct-to-Biology Accelerates PROTAC Synthesis and the Evaluation of Linker Effects on Permeability and Degradation. *ACS Med Chem Lett* 2022, *13* (7), 1182-1190.
17. Roberts, B. L.; Ma, Z. X.; Gao, A.; Leisten, E. D.; Yin, D.; Xu, W.; Tang, W., Two-Stage Strategy for Development of Proteolysis Targeting Chimeras and its Application for Estrogen Receptor Degraders. *ACS Chem. Biol.* 2020, *15* (6), 1487-1496.
18. Guo, L.; Zhou, Y.; Nie, X.; Zhang, Z.; Zhang, Z.; Li, C.; Wang, T.; Tang, W., A platform for the rapid synthesis of proteolysis targeting chimeras (Rapid-TAC) under miniaturized conditions. *European Journal of Medicinal Chemistry* 2022, *236*, 114317.
19. J. Mason, F. R., H. Wilders, D. Fallon https://github.com/thatchemistryguy/PyParse.
20. Mason, J. W., H; Fallon, D. J.; Thomas, R. P.; Bush, J. T.; Tomkinson, N. C. O.; Rianjongdee, F.;, Automated LC-MS Analysis and Data Extraction for High-Throughput Chemistry. *ChemRxiv 2023; This content is a preprint and has not been peer-reviewed.* 2023.
21. Ito, T.; Handa, H., Molecular mechanisms of thalidomide and its derivatives. *Proc Jpn Acad Ser B Phys Biol Sci* 2020, *96* (6), 189-203.
22. Bakshi, S.; McKee, C.; Walker, K.; Brown, C.; Chaudhry, G. R., Toxicity of JQ1 in neuronal derivatives of human umbilical cord mesenchymal stem cells. *Oncotarget* 2018, *9* (73), 33853-33864.
23. Burslem, G. M.; Smith, B. E.; Lai, A. C.; Jaime-Figueroa, S.; McQuaid, D. C.; Bondeson, D. P.; Toure, M.; Dong, H.; Qian, Y.; Wang, J.; Crew, A. P.; Hines, J.; Crews, C. M., The Advantages of Targeted Protein Degradation Over Inhibition: An RTK Case Study. *Cell Chem. Biol.* 2018, *25* (1), 67-77.
24. Hu, J.; Hu, B.; Wang, M.; Xu, F.; Miao, B.; Yang, C. Y.; Wang, M.; Liu, Z.; Hayes, D. F.; Chinnaswamy, K.; Delproposto, J.; Stuckey, J.; Wang, S., Discovery of ERD-308 as a Highly Potent Proteolysis Targeting Chimera (PROTAC) Degrader of Estrogen Receptor (ER). *J Med Chem* 2019, *62* (3), 1420-1442.
25. Schwinn, M. K.; Machleidt, T.; Zimmerman, K.; Eggers, C. T.; Dixon, A. S.; Hurst, R.; Hall, M. P.; Encell, L. P.; Binkowski, B. F.; Wood, K. V., CRISPR-Mediated Tagging of Endogenous Proteins with a Luminescent Peptide. *ACS Chem Biol* 2018, *13* (2), 467-474.
26. Riching, K. M.; Mahan, S. D.; Urh, M.; Daniels, D. L., High-Throughput Cellular Profiling of Targeted Protein Degradation Compounds using HiBiT CRISPR Cell Lines. *J Vis Exp* 2020, (165), e61787.
27. Valeur, E.; Bradley, M., Amide bond formation: beyond the myth of coupling reagents. *Chem Soc Rev* 2009, *38* (2), 606-31.
28. Wellaway, C. R.; Amans, D.; Bamborough, P.; Barnett, H.; Bit, R. A.; Brown, J. A.; Carlson, N. R.; Chung, C. W.; Cooper, A. W. J.; Craggs, P. D.; Davis, R. P.; Dean, T. W.; Evans, J. P.; Gordon, L.; Harada, I. L.; Hirst, D. J.; Humphreys, P. G.; Jones, K. L.; Lewis, A. J.; Lindon, M. J.; Lugo, D.; Mahmood, M.; McCleary, S.; Medeiros, P.;

17

Mitchell, D. J.; O'Sullivan, M.; Le Gall, A.; Patel, V. K.; Patten, C.; Poole, D. L.; Shah, R. R.; Smith, J. E.; Stafford, K. A. J.; Thomas, P. J.; Vimal, M.; Wall, I. D.; Watson, R. J.; Wellaway, N.; Yao, G.; Prinjha, R. K., Discovery of a Bromodomain and Extraterminal Inhibitor with a Low Predicted Human Dose through Synergistic Use of Encoded Library Technology and Fragment Screening. *J Med Chem* 2020, *63* (2), 714-746.

29. Goracci, L.; Desantis, J.; Valeri, A.; Castellani, B.; Eleuteri, M.; Cruciani, G., Understanding the Metabolism of Proteolysis Targeting Chimeras (PROTACs): The Next Step toward Pharmaceutical Applications. *J. Med. Chem.* 2020, *63* (20), 11615-11638.

30. Qin C Fau - Hu, Y.; Hu Y Fau - Zhou, B.; Zhou B Auid- Orcid: --- Fau - Fernandez-Salas, E.; Fernandez-Salas E Fau - Yang, C.-Y.; Yang Cy Fau - Liu, L.; Liu L Fau - McEachern, D.; McEachern D Fau - Przybranowski, S.; Przybranowski S Fau - Wang, M.; Wang M Fau - Stuckey, J.; Stuckey J Fau - Meagher, J.; Meagher J Fau - Bai, L.; Bai L Fau - Chen, Z.; Chen Z Fau - Lin, M.; Lin M Fau - Yang, J.; Yang J Fau - Ziazadeh, D. N.; Ziazadeh Dn Fau - Xu, F.; Xu F Fau - Hu, J.; Hu J Fau - Xiang, W.; Xiang W Fau - Huang, L.; Huang L Fau - Li, S.; Li S Fau - Wen, B.; Wen B Fau - Sun, D.; Sun D Fau - Wang, S.; Wang, S. A.-O., Discovery of QCA570 as an Exceptionally Potent and Efficacious Proteolysis Targeting Chimera (PROTAC) Degrader of the Bromodomain and Extra-Terminal (BET) Proteins Capable of Inducing Complete and Durable Tumor Regression. (1520-4804 (Electronic)).

31. Wang, C.; Zhang, Y.; Yang, S.; Chen, W.; Xing, D., PROTACs for BRDs proteins in cancer therapy: a review. *J Enzyme Inhib Med Chem* 2022, *37* (1), 1694-1703.

For Table of Contents Only